An Analytic Examination of the Effect of the Stratosphere on Surface Climate Through the Method of Piecewise Potential Vorticity Inversion

by

Irene W. Lee

B.A., Mathematics and Computer Science
Wellesley College, 1999

SUBMITTED TO THE DEPARTMENT OF EARTH, ATMOSPHERIC, AND PLANETARY SCIENCES IN PARTIAL FULFILLMENT OF THE REQUIREMENTS FOR THE DEGREE OF

MASTER OF SCIENCE IN ATMOSPHERIC SCIENCE

AT THE

MASSACHUSETTS INSTITUTE OF TECHNOLOGY

SEPTEMBER 2003

Signature of Author .....
Department of Earth, Atmospheric, and Planetary Sciences
August 8, 2003

Certified by .....
Raymond A. Plumb
Professor of Atmospheric Science
Thesis Supervisor

Accepted by .....
Maria T. Zuber
Head, Department of Earth, Atmospheric, and Planetary Sciences

An Analytic Examination of the Effect of the Stratosphere on Surface Climate Through the Method of Piecewise Potential Vorticity Inversion

by

Irene W. Lee

Submitted to the Department of Earth, Atmospheric,
and Planetary Sciences on August 8, 2003
in Partial Fulfillment of the Requirements for the
Degree of Master of Science in Atmospheric Science

ABSTRACT

An analytic study was performed to examine the effect of the stratosphere on the surface of the earth. The method of piecewise potential vorticity inversion was employed in the diagnosis of the magnitude of and dynamics behind the stratosphere-surface link in both the transient and stationary cases.

The potential vorticity inversion results in both the transient and stationary models indicated that the stratosphere possesses a significant effect at the surface of the earth. It was determined that, compared to the stratosphere as a whole, it was primarily the lower stratosphere that had the most significant impact at the surface of the earth. The results of this analytic study therefore indicate that in modeling the surface of the earth, the dynamics detailed here between the lower stratosphere and surface must be included for the modeled surface weather or climate simulations to be accurate.

Thesis Supervisor: Raymond A. Plumb
Title: Professor of Atmospheric Science

Acknowledgements

First and foremost, I would like to thank my mother and sister for all their support. I would also like to thank my advisor, Professor Plumb, and the financial support of the ASEE/NDSEG Fellowship.

I. INTRODUCTION

In the atmospheric sciences the atmosphere has been divided into five distinct layers for study: the troposphere, stratosphere, mesosphere, thermosphere and exosphere. As residents of the surface of the earth, it is ultimately the weather occurring in the lowest part of the troposphere that has the greatest impact on daily life. Being able to accurately predict the weather hours, days or weeks in advance can mean advantages that range anywhere from an answer to the mundane "will I need an umbrella today" to critical predictions such as the likelihood of a major flood, equaling large sums of money and more importantly human lives. Therefore, from the practical point of view of wanting to be able to accurately predict surface weather for its impact on human life, any means of improving current forecasting skill is welcome.

Many surface weather forecasting models currently limit the simulation of the atmosphere to the troposphere alone. As a result of the relatively volatile dynamics in the troposphere, surface weather forecasts generally possess little skill beyond the range of one week. However, there has been much discussion recently as to the possibility that, in fact, the stratosphere may also play a significant role in determining the weather at the surface. Unlike the troposphere, the stratosphere evolves on slower time-scales on the order of weeks and months rather than days. Therefore, if the stratosphere does possess a sort of downward control on the troposphere, the addition of a properly simulated stratosphere to forecasting models, although computationally expensive, would certainly result in an improvement in both the accuracy and range of surface weather forecasts. On the other hand, if it can be shown that there is no such stratosphere-troposphere link then it could be

known that surface weather forecasting models could safely exclude simulation of a stratosphere without any loss of skill. Such knowledge, one way or the other, would mean an increased confidence and potential improvement in the methods employed by forecasting models and, consequently, in the accuracy and range of the surface weather forecasts they produce as well.

From an atmospheric dynamics standpoint, it is well known that information in the atmosphere can be transmitted upward [Charney and Drazin, 1961]. For example, the dynamics of the stratosphere are known to depend strongly on the surface of the earth and troposphere by means of upward propagating planetary waves. However, downward communication in the atmosphere is less well understood and in fact there is no one widely accepted mechanism to explain such a phenomenon, if it exists. Proof of a significant effect of the stratosphere on the surface or evidence to the contrary would thus serve to either help reveal further or confirm the precise dynamics occurring between the stratosphere and the surface. Examining the existence of a link between the stratosphere and the surface of the earth is thus of real value in terms of increasing the comprehension of the inner dynamical workings of the atmosphere and its potential for downward communication. Therefore, studying the problem of stratosphere-troposphere coupling is of great importance from both the real-world and atmospheric dynamics perspectives.

In studying the possible link between the stratosphere and the troposphere it is useful to examine it under the context of the Arctic Oscillation (AO). The AO was first defined by Thompson and Wallace [1998] as the leading empirical orthogonal function (EOF) of the wintertime monthly mean sea-level pressure (SLP) anomaly field in the

Northern Hemisphere. It is important to note, however, that the AO is an extremely robust pattern and is not restricted to either winter or surface data. In fact, it can be recovered through a variety of different analysis techniques and data sets [Baldwin, 2000]. Baldwin and Dunkerton [1999], for example, recovered the pattern of the AO using the geopotential height fields at five levels throughout the troposphere and stratosphere. It should also be noted that there has been much discussion in the literature recently as to the relationship and confusion between the AO, the Northern Annular Mode (NAM), and the North Atlantic Oscillation (NAO). Although there is still some dispute, the general consensus seems to be as follows. As a result of its strong zonal symmetry, the AO phenomenon is sometimes referred to as the NAM [Thompson and Wallace, 2000], and so the AO and NAM acronyms may be considered interchangeable. The NAO represents the oscillation of low and high SLP over the Atlantic Basin. Therefore, the NAO can be thought of as the regional counterpart of the AO, as the AO encompasses the entire Northern Hemisphere [Wallace, 2000; Wallace and Thompson, 2002]. In other words, the AO, NAM, and NAO can be regarded as essentially describing the same phenomenon of an alternation between anomalously high and low SLP over the polar and mid-latitude regions of the Northern Hemisphere. Hereafter, this phenomenon will be referred to as the AO.

Part of the usefulness of the AO stems from the fact that it represents a significant portion of the atmospheric variability in the Northern Hemisphere, approximately 22% of the variance in SLP [Thompson and Wallace, 1998], second only to the seasonal cycle [Baldwin, 2000]. An AO index has been defined such that a high index represents the state of anomalously low SLP over the polar regions and anomalously high SLP over the mid-

latitudes, and a low index vice versa. Several characteristics of a high AO index phase include increased surface westerlies over the North Atlantic, and warmer and wetter weather over northern Europe. The opposite generally occurs during low index phases, with an increased likelihood of extreme cold temperatures [Wallace and Thompson, 2002]. The phase of the AO has also been shown to have a significant impact on storm track placement in the Northern Hemisphere [Hurrell, 1995; Baldwin and Dunkerton, 2001]. Therefore, it is clear that any ability to accurately predict the phase of the AO would have a significant impact on the accuracy of Northern Hemisphere surface climate forecasts.

The signal of the AO at the surface of the earth has also been shown to be statistically correlated to the strength of the polar vortex in the stratosphere in the Northern Hemisphere [Baldwin *et al.*, 1994; Perlwitz and Graf, 1995; Kuroda and Kodera, 1999; Baldwin and Dunkerton, 2001]. During high index phases of the AO, the westerly winds of the polar vortex tend to be anomalously strong, while the opposite tends to be true during low AO index phases. The link between the strength of the polar vortex and the AO index at the surface is most pronounced during the late winter months [Wallace and Thompson, 2002]. It is precisely this link that makes the AO the ideal context under which to study the possibility of a stratosphere-troposphere connection. In addition to this, in terms of potential vorticity inversion analyses of the potential effect of the stratosphere on the earth's surface, the potential vorticity anomaly associated with the AO and polar vortex in the stratosphere is large in both magnitude and spatial scale and has, therefore, the greatest chance of having an associated signal that reaches all the way down to the surface

of the earth [Black, 2002]. Note that the method of potential vorticity inversion will be described in further detail in Section II.

Baldwin and Dunkerton [1999] showed that the phase of the AO has a tendency to propagate downward from the stratosphere into the troposphere and even to the surface of the earth with an average descent period of three weeks. However, the downward propagation of the AO phase is not always present, and when present has a strongly variable descent rate that can range anywhere from a few days to over a month. At times, in fact, the phase of the AO actually occurs either simultaneously in both the stratosphere and troposphere or is even seen to propagate upwards from the troposphere into the stratosphere. [Baldwin and Dunkerton, 2001] Moreover, it cannot be determined if the seeming downward propagation is the result of a cause and effect of the stratosphere acting on the troposphere. It is possible, as suggested by Baldwin and Dunkerton [1999], that the apparent downward propagation is simply the result of like AO phases occurring in the stratosphere and troposphere somewhat coincidentally resulting in mutual amplification, which the highly variable rate of descent would seem to support. Nonetheless, the apparent downward propagation occurs often enough that it can still be of use in predicting the phase of the AO at the surface of the earth on the order of weeks, which may prove useful in improving the accuracy of medium-range surface weather forecasts [Baldwin, 2000; Kerr, 2001]. In fact, during stratospheric events with large accompanying AO signals, such as major stratospheric warmings consisting of a significant weakening or complete breakdown of the polar vortex, there is a greater likelihood that the AO pattern will descend from the stratosphere into the troposphere and to the surface than in cases

where the magnitude of the AO signal is relatively small [Baldwin and Dunkerton, 1999]. The findings here of Baldwin and Dunkerton are intriguing and certainly indicate that a significant dynamical link between the stratosphere and troposphere is probable, but precisely what that link might consist of is as yet unclear.

The subject of downward communication in the atmosphere is a relatively new topic and it has been widely disputed whether it is even possible for the stratosphere to have a significant effect on the surface of the earth. For one thing, the small mass of the stratosphere, as compared to the relatively large mass of the troposphere, requires that any perturbations of stratospheric origin must then have a sufficiently large magnitude in order to be able to penetrate through the troposphere and still have a significant signal at the surface of the earth. Another point that argues against the possibility of downward communication is the fact that the majority of communication in the atmosphere is in the upwards direction, by way of planetary waves which propagate upward from the surface of the earth and troposphere into the stratosphere, and not vice versa. [Wallace and Thompson, 2002] However, recent published findings such as the studies showing the downward propagation of the AO [eg. Baldwin and Dunkerton, 1999, 2001] and anomalies of other key meteorological fields, such as zonal wind anomalies [eg. Kodera et al, 1990], from the stratosphere into the troposphere and down to the surface of the earth, have made it increasingly evident that likely some link exists between the stratosphere and troposphere. As a result, there have been several theories proposed to explain the mechanics behind the apparent dynamical stratosphere-troposphere link. These range from supporting the theory of direct downward influence, or a direct forcing of the stratosphere

on the troposphere, to that of an indirect or feedback theory in which the apparent downward communication from the stratosphere is ultimately the manifestation of events that originated in the troposphere. Detailed here will be several of those theories.

Plumb and Semeniuk [2003] have proposed a mechanism based upon local wave, mean-flow interaction, similar to the mechanism regarded as driving the alternating easterly-westerly zonal wind phenomenon of the quasi-biennial oscillation (QBO). In both one- and three-dimensional models, it was shown that the downward propagation of extratropical zonal wind anomalies from the stratosphere into the troposphere could be achieved solely through fluctuations of Rossby wave activity in the troposphere. Essentially, Rossby waves originating in the troposphere propagate upward into the stratosphere until they reach a critical level at which they deposit their associated easterly-momentum, thus forcing the mean flow and lowering the critical level, and so on, giving the appearance of downward propagating zonal wind anomalies. This theory explains that, though the extratropical zonal wind anomalies appear to propagate downward from the stratosphere to the troposphere, it is not the result of a direct forcing of the stratosphere on the troposphere, but rather a manifestation of a stratospheric response to upward forcing by the troposphere. These findings suggest that, therefore, a similar indirect forcing mechanism may also be responsible for the observed downward propagation of the AO.

Hartley et al. [1998] employed the method of piecewise potential vorticity inversion to show that major distortions in the stratospheric polar vortex can have a significant effect on key meteorological fields in the upper troposphere. It was found that the stratospheric potential vorticity anomalies associated with major polar vortex distortion

events were responsible for inducing, on average, 34% of the geopotential height anomalies at the tropopause, with the majority of this due to the potential vorticity redistribution in the lower and middle stratosphere. It was concluded that the stratosphere has a significant direct feedback upon the troposphere, larger than previously thought, and that therefore a more realistic representation of related stratospheric processes in atmospheric models would result in a significant improvement in the accuracy of tropospheric simulations.

Black [2002], expanding on the study of Hartley et al. [1998], used the method of piecewise potential vorticity inversion to show that the stratosphere has a significant effect on the AO signal down to the surface of the earth. He found that at high latitudes north of 40° N, the potential vorticity anomalies associated with the wintertime polar vortex in the lower stratosphere below 30 mb resulted in a significant westerly zonal wind signal at the earth's surface. Upon closer examination of the potential vorticity anomalies associated with the observed downward propagation of the AO signal from the stratosphere to the surface of the earth, Black concluded that in such cases the lower stratosphere has a direct downward impact on surface climate. He suggested that an indirect mechanism is initially responsible for moving the AO signal from the middle stratosphere down to the lower stratosphere through a feedback mechanism involving the alteration of the propagation characteristics of tropospheric planetary waves, in agreement with indirect feedback theories [eg. Kuroda and Kodera, 1999]. At this point a direct forcing mechanism takes over, where the AO associated potential vorticity anomaly in the lower stratosphere dynamically induces an associated potential vorticity anomaly in the troposphere, creating

significant anomalies in key meteorological fields at the surface of the earth. Though Black suggests that the lower stratosphere has a direct downward influence on the earth's surface under the context of the AO, he does point out that on short intraseasonal time scales the mechanism could more properly be regarded as a dynamical feedback, since the initial changes in potential vorticity in the stratosphere are ultimately due to changes in the troposphere. However, on longer timescales the stratospheric potential vorticity anomalies may be the result of local radiative processes, in which case a direct downward forcing mechanism would be responsible for the propagation of the AO signal from the stratosphere to the earth's surface. This leads to the conclusion that the stratosphere can indeed have a direct impact on the surface of the earth, and that it should therefore be adequately modeled in any attempts to accurately forecast surface climate.

Thus, it is clear that at present no final consensus has been reached on the precise dynamics behind the observed downward propagation of the AO and related fields from the stratosphere to the troposphere. Nonetheless, it is readily apparent that communication is occurring between the stratosphere and troposphere that is not well understood, whether the underlying mechanics turn out to be comprised of a direct downward effect, an indirect feedback, or perhaps a combination of the two. Therefore, in order to fully understand the dynamics of what is occurring, it is necessary to continue studying further the interaction taking place between the stratosphere and troposphere. In all likelihood, such a continued effort will eventually reveal enough details of the stratosphere-troposphere link to finally allow for the construction of a complete dynamical picture of the mechanism responsible for the downward communication in the atmosphere. This thesis will therefore proceed to

examine the stratosphere-troposphere link under the context of the AO in an attempt to uncover additional details of the mechanism behind downward communication in the atmosphere, and how this in turn affects the present understanding of a stratospheric effect on surface weather and climate.

II. METHOD

In a similar approach to that employed by Hartley et al. [1998] and Black [2002], this study will use the method of piecewise potential vorticity inversion under the context of the AO to examine the relative effect of the stratosphere on the surface of the earth. However, unlike the aforementioned studies, the solutions here will be obtained analytically rather than numerically. The first part of this study will focus on how potential vorticity anomalies in the stratosphere affect the weather at the surface in the transient case, i.e. for relatively instantaneous time scales of O(~days), during a simulated major stratospheric warming. The second half of the study will then focus on modeling the associated effect the stratosphere has on surface climate in the stationary case, i.e. for averaged time scales greater than O(~months). The term "weather" will be used to describe the associated surface meteorological fields in the transient solution, while "climate" will be used in the stationary case.

Potential vorticity is a useful parameter to examine in part for the fact that a multitude of other key meteorological fields, such as wind and temperature fields, can be deduced from this single field via its relationship with geopotential height. It is particularly useful in studying the effect of the stratosphere on the surface of the earth for

the following reasons. The stratospheric polar vortex is very conducive to being characterized as a deep and vast pool of positive potential vorticity in the Northern hemisphere. Analogous to how a local electric charge induces a non-local electric field, the larger the magnitude and size of a potential vorticity anomaly, the farther reaching its non-local effect will be [Bishop and Thorpe, 1994]. Since the complete breakdown of the polar vortex during a major warming can be represented as a deep and large stratospherically-located negative potential vorticity anomaly, the greatest chance of a significant non-local effect being able to reach down to the earth's surface is here. In other words, if the stratosphere can affect the surface of the earth, the most likely chance of observing this interaction would be during a significant distortion of the polar vortex, such as a major warming. And, by examining it through the perspective of potential vorticity, the magnitude of the associated surface effect can be gauged by, for example, deducing the zonal wind field at the surface.

The method of piecewise potential vorticity inversion [Davis and Emanuel, 1991; Davis, 1992] allows the relative effects of subsets or "pieces" of the whole potential vorticity anomaly field on a single non-local field to be diagnosed separately by the superposition principle, using the electrostatics analogy. In general, the relationship between potential vorticity and geopotential height is nonlinear which leads to ambiguity in the solutions of piecewise inversions. However, under the assumption of quasi-geostrophy (QG), the potential vorticity-geopotential height relationship becomes linear and thus all piecewise inversions become unambiguous. In other words, under QG theory the solution obtained by inverting the entire potential vorticity anomaly field as a whole

will be identical to the solution obtained by dividing the field into subsets and summing the individual solutions of those subsets. The theory of QG is valid for atmospheric motions in which the ratio of the horizontal advection terms in the momentum equations to the Coriolis term is small, i.e. for small Rossby number values. This holds away from the equator and below approximately 10 mb (30 km) [Hartley *et al.*, 1998], which are the regions of primary concern in this study. Therefore, QG will be assumed and from here on PV will refer to quasi-geostrophic potential vorticity.

Using the method of piecewise PV inversion, the stratosphere may be divided into a wide range of layers of varying thicknesses, heights, and associated PV anomaly magnitudes. Then, under the assumption of QG, the subsequent unambiguous piecewise PV inversions of each practically chosen layer will allow aspects of the dynamical interaction between the stratosphere and the surface of the earth to be revealed. The following sections will proceed to detail the setup and analytic solutions for the transient and stationary models, and the results of the case studies performed.

III. TRANSIENT SOLUTION MODEL

The effect of the stratosphere on the surface will first be examined in a model of the transient solution. The setup to solving this problem analytically involves inducing to a system at rest an isolated PV perturbation in an infinite layer above a certain level in the stratosphere and solving for the associated zonal wind and temperature anomalies at the surface of the earth. Once the general solution has been obtained, it is then straightforward to repeatedly solve for the surface solution for different magnitudes of the PV perturbation

and different heights above which the perturbation resides. Since this is being performed under the assumption of QG, the resulting set of solutions may then be added and subtracted at will to give an infinite set of solutions representative of any variation in stratospheric PV perturbation strength and height. By making useful and realistic choices for the magnitudes and heights of the PV perturbations, an analytic diagnosis may be made of how the stratosphere interacts with the surface during, say, a major stratospheric warming and truly a wide variety of other atmospheric situations using the method of piecewise PV inversion.

The model will be set up using log-pressure coordinates on a beta-plane in a channel of width L. Along with the QG assumption, it will be assumed that the system is in an inviscid and adiabatic state and that there are no variations in the zonal direction. These assumptions may not necessarily be realistic in terms of the real-world atmosphere, but they prove to be useful here in terms of keeping the analytic problem simple and its solution comprehensible. Provided here in Table 1 is a list of the relevant constants and variables for reference.

f_0	= Coriolis parameter centered at 45° N	=	1.031×10^{-4} s^{-1}
g	= acceleration due to gravity	=	9.81 m s^{-2}
T_T	= average temperature in the troposphere	=	228 K
T_S	= average temperature in the stratosphere	=	212 K
N_T	= Brunt-Väisälä frequency of the troposphere	=	1.34×10^{-2} s^{-1}
N_S	= Brunt-Väisälä frequency of the stratosphere	=	2.19×10^{-2} s^{-1}
H_T	= scale height in the troposphere	=	6.21×10^{3} m

H_S	= scale height in the stratosphere	=	6.69×10^3 m
L	= channel width equivalent to 60° in latitude	=	6.67×10^6 m
H_{TR}	= height of the tropopause	=	1.2×10^4 m
H_{PV}	= lower boundary of PV layer	=	constant *(controlled)*
p	= pressure	=	[mb]
ρ	= density	=	[kg m^{-3}]
z	= log-pressure height coordinate	=	$- H_{T,S} \ln p$ [m]
q_p'	= pseudo-potential vorticity anomaly	=	[m^2 s^{-1} K kg^{-1}]
Q	= magnitude of PV anomaly	=	constant *(controlled)*
m	= mode of PV anomaly	=	integer *(controlled)*
ψ'	= geopotential height anomaly	=	[m]
u_s'	= surface zonal wind anomaly	=	[m s^{-1}]
$[\ ]_T$	= layer from surface to H_{TR}		
$[\ ]_S$	= layer from H_{TR} to H_{PV}		
$[\ ]_{PV}$	= layer from H_{PV} to infinity		

Table 1. Constants and Variables

In order to simulate an isolated PV perturbation in the stratosphere, it will be assumed that waves in the model are only produced at the solid surface of the earth, and therefore not anywhere in the atmosphere. Such a flux of waves up from the surface may be thought of as the result of topography in the real world, for example. Next, it will be assumed that these waves propagate upwards from the surface to a certain level in the stratosphere, H_{PV} in this model, above which they entirely dissipate. This complete wave

dissipation results in a stratospheric redistribution of PV in the layer of dissipation, i.e. the infinite layer above H_{PV}. It should be noted that if, for example, wave formation were chosen to occur in the troposphere instead of, or as well as, at the solid surface, just as wave dissipation in the stratosphere results in anomalous PV, wave production in the troposphere would result in an oppositely-signed PV perturbation of proportionate magnitude at the level of formation, and consequently undesired internal atmospheric PV anomaly interactions. Therefore, although it is somewhat unrealistic to assume that there is no wave formation in the atmosphere as the result of say, heating, by limiting wave creation to the solid surface the model will have only the single PV anomaly isolated in the stratosphere, as desired for this study. This setup allows the analysis of the link between the stratosphere and surface to remain straightforward and unobscured by internal PV anomaly interactions.

During a major stratospheric warming, the breakdown of the polar vortex is represented by a weakening of the previously strong circumpolar westerly winds. This will be represented by a decrease in PV in the stratosphere near the pole, or equivalently as a negative PV perturbation. To simulate this analytically, the induced PV perturbation in the stratosphere will have the form

$$q_p' = Q\cos\frac{m\pi y}{L}. \tag{1}$$

The reasons behind the choice of a cosine representation for the PV perturbation are twofold. The first reason is that PV must be conserved on each z surface, and so the anomalous PV must integrate to zero over the hemisphere. The second reason stems from the imposed lateral boundary conditions at the two rigid channel walls which state that the

anomalous zonal wind u' must be zero at $y = 0, L$. Since it is assumed that the solution of ψ' will vary meridionally as q_P' in Equation 1, i.e. as $\cos\frac{m\pi y}{L}$, then since

$$u' = -\frac{\partial \psi'}{\partial y}, \tag{2}$$

these two lateral boundary conditions are satisfied by the cosine representation of the PV perturbation. For m = 1, the resulting PV perturbation will have the form as shown in Figure 1.

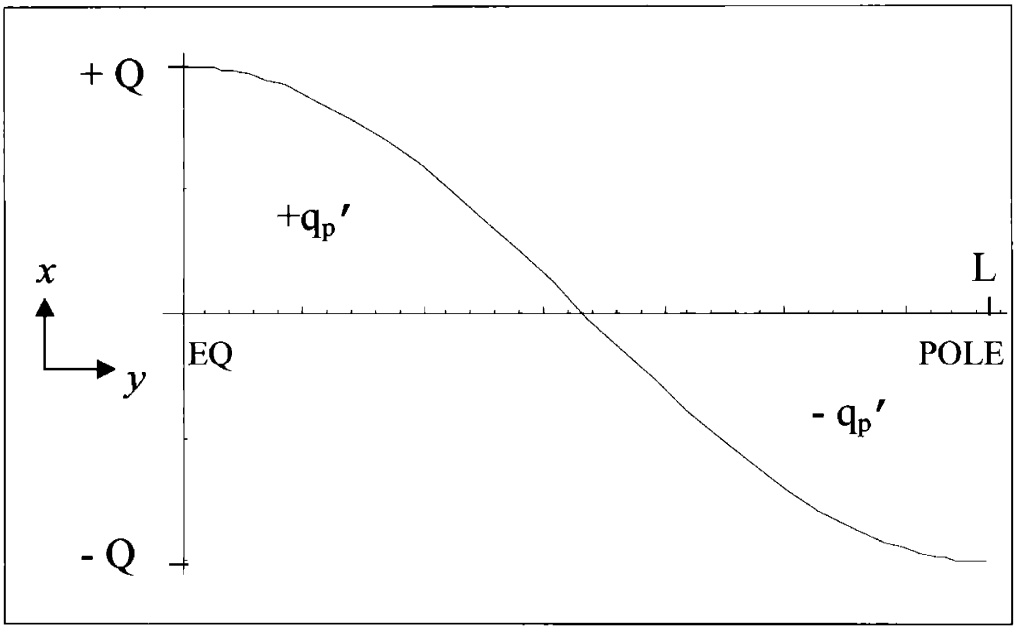

Figure 1. PV anomaly for $m = 1$

It is also possible to solve this problem for multiple values of m, which will allow the construction of any linear combination of solutions in order to simulate a wide variety of PV perturbation shapes in the stratosphere while still conserving PV. The QG PV equation is

$$q_p' = \frac{\partial^2 \psi'}{\partial x^2} + \frac{\partial^2 \psi'}{\partial y^2} + \frac{f_0^2}{N^2}\left(\frac{\partial^2 \psi'}{\partial z^2} - \frac{1}{H}\frac{\partial \psi'}{\partial z}\right), \tag{3}$$

with the appropriate T and S subscripts applied to N and H in the troposphere and stratosphere respectively. The atmospheric model will be divided into three regions: one bounded by the surface of the earth and the tropopause, the next by the tropopause and H_{PV}, and the last region infinite above H_{PV}. The anomalous PV, q_p', is set to be zero everywhere except for the infinite region in the stratosphere above the height H_{PV}. The objective is to solve the QG PV equation for ψ' with this atmospheric distribution of PV in order to obtain the zonal wind and temperature anomaly fields at the earth's surface. Therefore, q_p' will be inverted for a solution of ψ' in each of these three regions, with boundary conditions applied at the surface and above. At the surface of the earth, PV is represented by variations in temperature. Because it is assumed that there is no anomalous PV in the model except for the region in the stratosphere, there may not be any perturbations in PV at the surface, and consequently no perturbations in temperature at the surface either, $T' = 0$, and so the surface boundary condition is

$$\frac{\partial \psi'}{\partial z} = 0, \tag{4}$$

since

$$T' = \frac{f_0 T_{S,T}}{g}\frac{\partial \psi'}{\partial z}. \tag{5}$$

It is assumed that the solutions decay exponentially with height, so the upper boundary condition at the top of the model is that all solutions must go to zero as $z \to \infty$. However, the two boundary conditions detailed above are insufficient to uniquely solve for ψ'.

Therefore, matching conditions must also be applied at the two interfaces between the three regions in order to obtain a unique solution for ψ'. The first interfacial matching condition stems from the fact that since pressure is a continuous function in the atmosphere, ψ' must also be continuous. For simplicity, it will be assumed in the transient solution model that the initial background state of temperature is a continuous function. Then, by applying this to the thermodynamic equation, combined with the previously mentioned assumptions of the initial state of the model atmosphere at rest and no variations in the zonal direction, the second matching condition may be determined. The two interfacial matching conditions are therefore

$$\text{i.} \qquad \psi'_{above} = \psi'_{below} \qquad \text{at} \quad z = H_{TR},\, H_{PV} \tag{6}$$

$$\text{ii.} \qquad \frac{\partial \psi'}{\partial z}_{above} = \frac{\partial \psi'}{\partial z}_{below} \qquad \text{at} \quad z = H_{TR},\, H_{PV}. \tag{7}$$

A diagram of the model setup is depicted as follows in Figure 2.

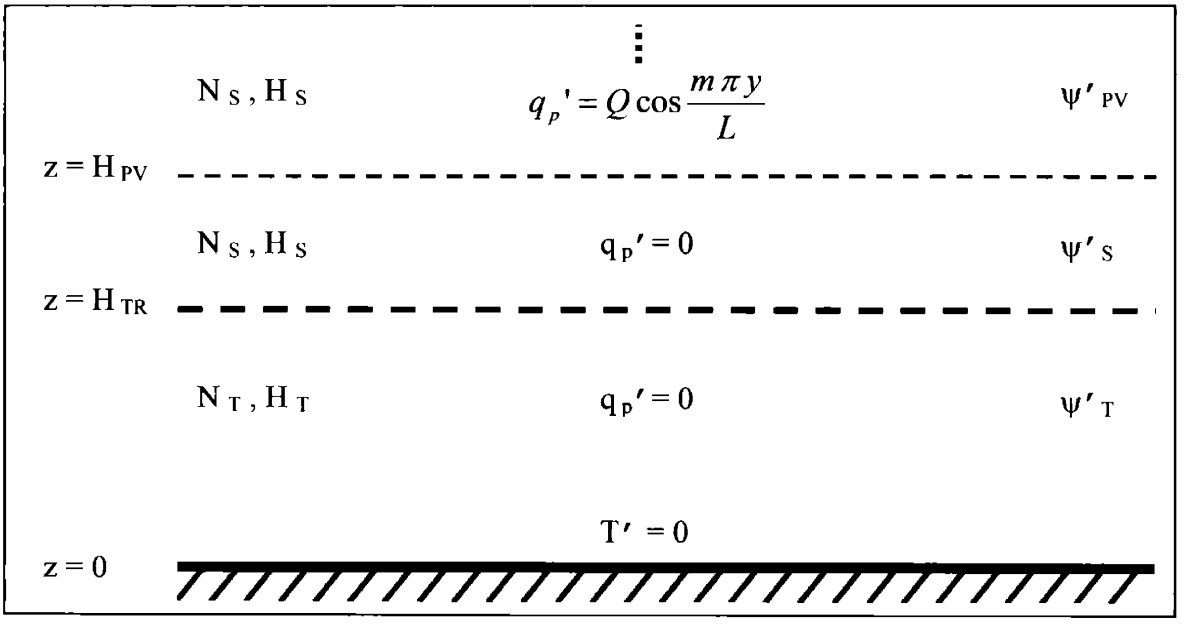

Figure 2. Transient solution model setup

It will be assumed that the solutions have the form

$$\psi'_{T,S,PV} = F_{T,S,PV}(z)\cos\frac{m\pi y}{L}. \tag{8}$$

Inverting the q_p' equations for ψ' in each region and applying the relevant boundary and interfacial matching conditions gives the following solution for ψ'.

$$\psi' = \left(\cos\frac{m\pi y}{L}\right) * \begin{cases} c_1 e^{az} - \dfrac{QL^2}{m^2\pi^2} & for \quad z \geq H_{PV} \\ c_2 e^{az} + c_3 e^{bz} & for \quad H_{TR} \leq z \leq H_{PV} \\ c_4\left(e^{dz} - \dfrac{d}{c}e^{cz}\right) & for \quad 0 \leq z \leq H_{TR} \end{cases}, \tag{9}$$

where

$$a(b) = \frac{1}{2H_S} \; - \; (+)\sqrt{\frac{1}{4H_S^2} + \frac{N_S^2 m^2 \pi^2}{f_0^2 L^2}}, \tag{9a}$$

$$c(d) = \frac{1}{2H_T} \; - \; (+)\sqrt{\frac{1}{4H_T^2} + \frac{N_T^2 m^2 \pi^2}{f_0^2 L^2}}, \tag{9b}$$

$$c_1 = c_2 + c_3 e^{H_{PV}(b-a)} + \frac{QL^2}{m^2\pi^2} e^{-aH_{PV}}, \tag{9c}$$

$$c_2 = \left[\frac{(b-d)e^{H_{TR}(b+d)} - d\left(\dfrac{b}{c}+1\right)e^{H_{TR}(b+c)}}{(a+d)e^{H_{TR}(a+d)} - d\left(\dfrac{a}{c}+1\right)e^{H_{TR}(a+c)}}\right] * c_3, \tag{9d}$$

$$c_3 = \frac{QL^2}{m^2\pi^2}\frac{a}{b-a}e^{-bH_{PV}}, \tag{9e}$$

and

$$c_4 = \frac{ac_2 e^{a H_{TR}} + bc_3 e^{b H_{TR}}}{d\left(e^{d H_{TR}} - e^{c H_{TR}}\right)}. \tag{9f}$$

The wind and temperature perturbation fields throughout the atmosphere and at the surface of the earth may now be solved for with the above solution of ψ', using Equations 2 and 5 respectively. However, it should be noted that the imposed surface boundary condition, given in Equation 4, requires that the temperature perturbation field always be zero at the surface. Therefore, in this model it is actually more useful to examine the zonal wind anomaly field at the surface as a measure of surface weather response to stratospheric change. Nonetheless, it may still be of interest to see how the temperature perturbation profile changes throughout the atmosphere in response to changes in the stratosphere. Shown here in Figures 3-6 are the perturbation PV, temperature, and zonal wind fields for a typical solution, calculated for Q = 1.0 x 10^{-4} m^2 s^{-1} K kg^{-1} and H_{PV} = 15 km. Note that the value of Q = 1.0 x 10^{-4} m^2 s^{-1} K kg^{-1} is approximately the largest magnitude Q may realistically have in the atmosphere as determined from Figure 1 in the study by Black [2002], and has been chosen in order to obtain the largest realistic related surface signal.

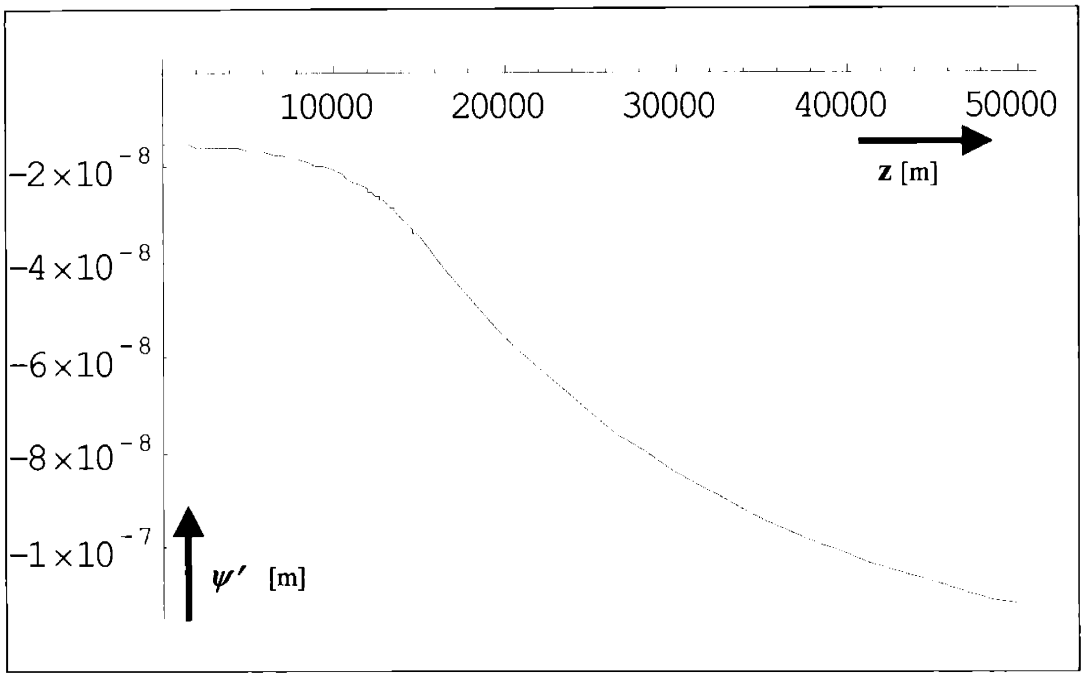

Figure 3. Geopotential height anomaly (ψ') height profile at $y = L/2$

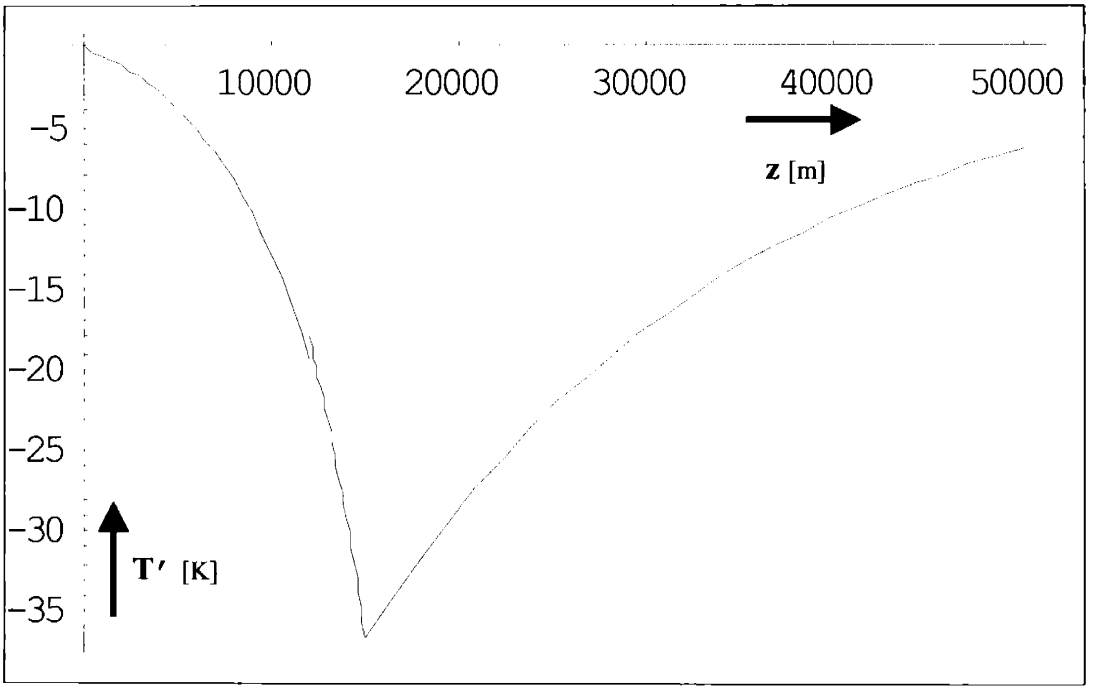

Figure 4. Temperature anomaly (T') height profile at $y = 0$

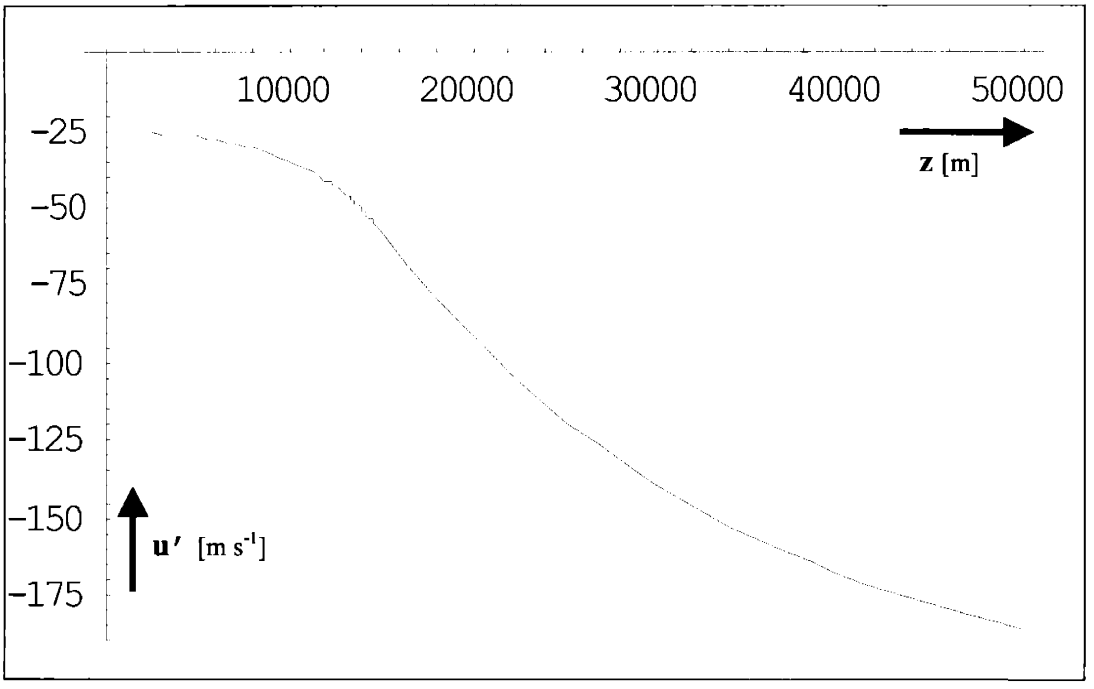

Figure 5. Zonal wind anomaly (u') height profile at $y = L/2$

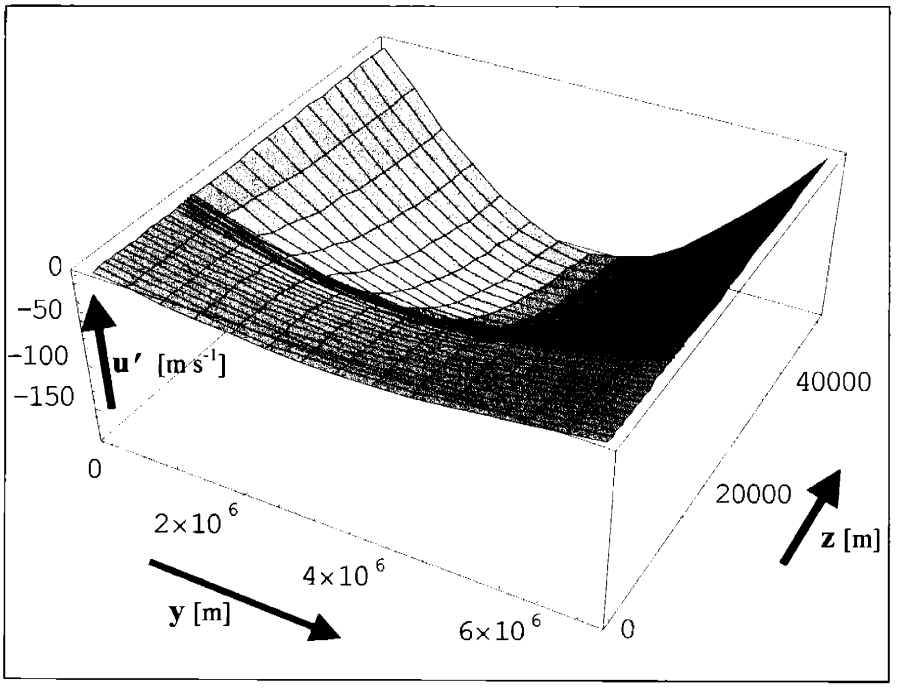

Figure 6. Zonal wind anomaly (u') field

Note that in Figure 4 there is a slight discontinuity in temperature at the tropopause, and this is the result of the average temperature profile used, which consists of a discontinuous jump from T_T = 228 K to T_S = 212 K at the tropopause, H_{TR} = 12 km. Also, in Figure 6 note that the zonal wind anomaly is zero at $y = 0, L$ as required by the imposed lateral boundary conditions at the two rigid walls. The reason behind the solutions for the geopotential height and zonal wind anomalies having the same basic shape with height can be seen in Equation 2, i.e. the solutions only differ in height by a constant. By comparison, the somewhat V-shape of the temperature profile in Figure 4 is a result of the $\frac{\partial \psi'}{\partial z}$ factor in Equation 5.

IV. TRANSIENT SOLUTION MODEL – Case 1

In this case, it will be examined how PV perturbation height and thickness in the stratosphere affects the associated signal in anomalous zonal wind at the surface in the transient solution model. This may be achieved by inducing a fixed constant PV perturbation in the infinite layer above H_{PV}, and then repeatedly solving for the associated surface zonal wind anomalies with changing heights of H_{PV}. Because the transient solution was found under the assumption of QG, the infinite PV anomaly layers and resulting surface zonal wind anomaly solutions may be added and subtracted unambiguously in order to obtain solutions for finite layers of any thickness and height. Since the magnitude of the PV anomaly is being held constant, this essentially gives the solution for the change in surface zonal wind anomaly as a PV perturbation's height and thickness changes throughout the stratosphere.

As previously stated, the maximum realistic value for a stratospheric PV perturbation is approximately $Q = 1.0 \times 10^{-4}$ m^2 s^{-1} K kg^{-1}, and so this is the value that will be used here. It should be noted that, although the QG approximation does not hold above 30 km, results above this height are given for completeness. In order to assess the effect PV anomaly height has on the associated non-local effect at the earth's surface, the associated height profiles of ψ', T', u', and u' fields for two different layers are shown in Figures 7-10 respectively. The first layer is located between 13-14 km near the tropopause in the lowermost part of the lower stratosphere, and the second layer is located between 26-27 km in the lowermost part of the middle stratosphere. The two layers have been chosen to both have a thickness of one kilometer for ease of graphical comparison. The heights of the two layers have been chosen not only to exhibit how PV anomaly height affects perturbation fields of interest, but also to allow an assessment to be made of the relative impacts the lower and middle stratosphere have on the weather at the surface.

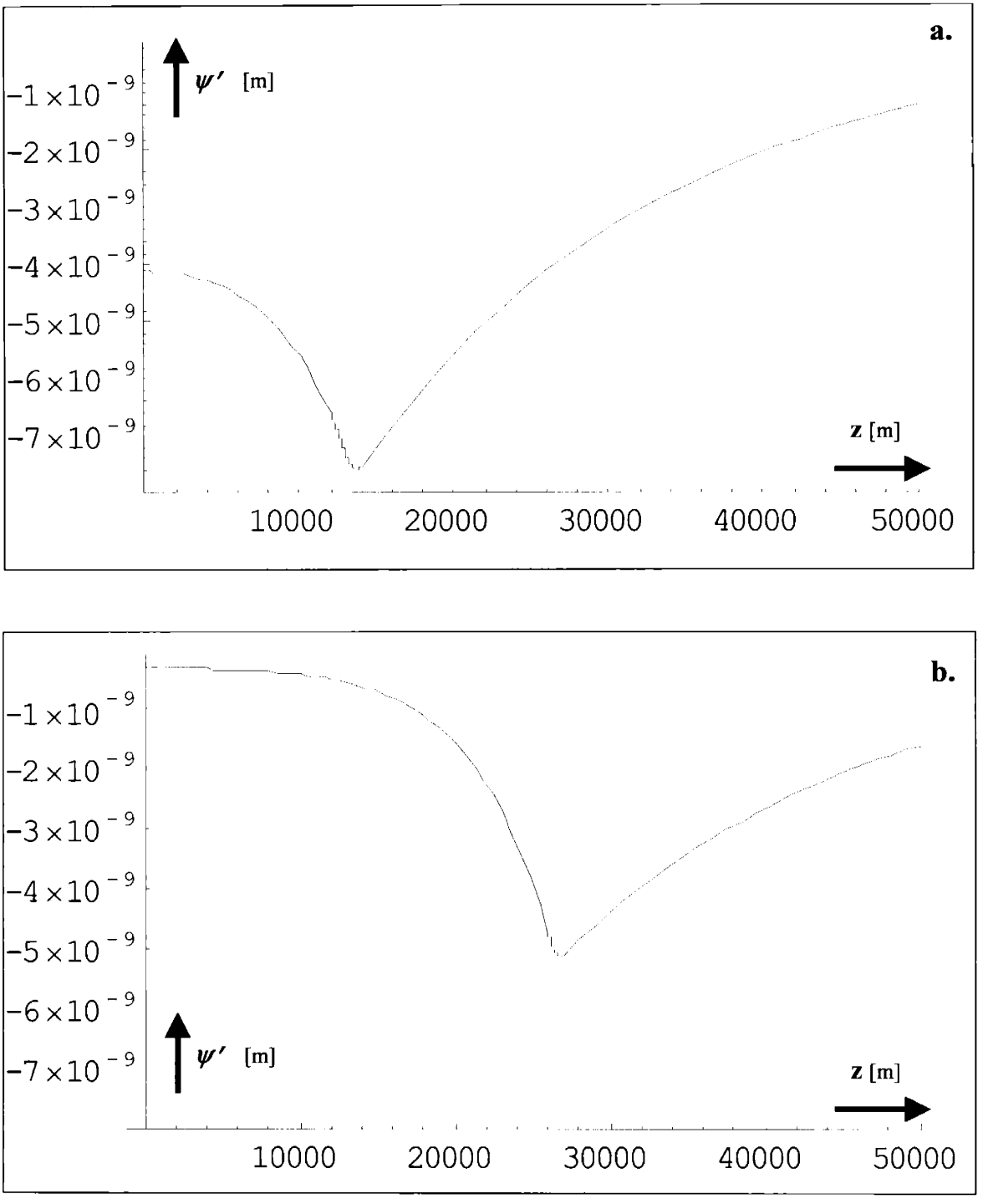

Figure 7. Geopotential height anomaly (ψ') height profile at $y = L/2$

a. 13 – 14 km Layer
b. 26 – 27 km Layer

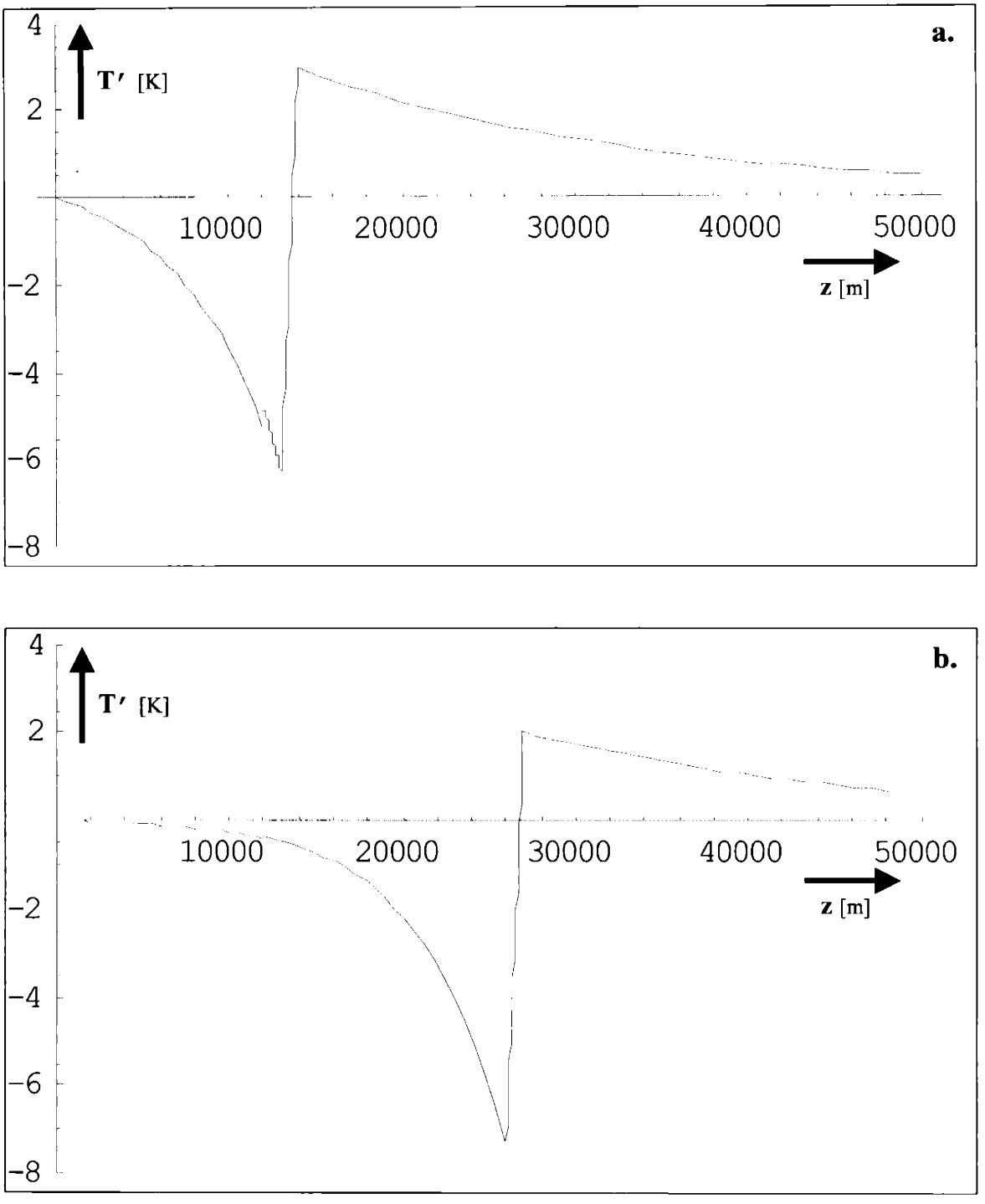

Figure 8. Temperature anomaly (T') height profile at $y = 0$

a. 13 – 14 km Layer
b. 26 – 27 km Layer

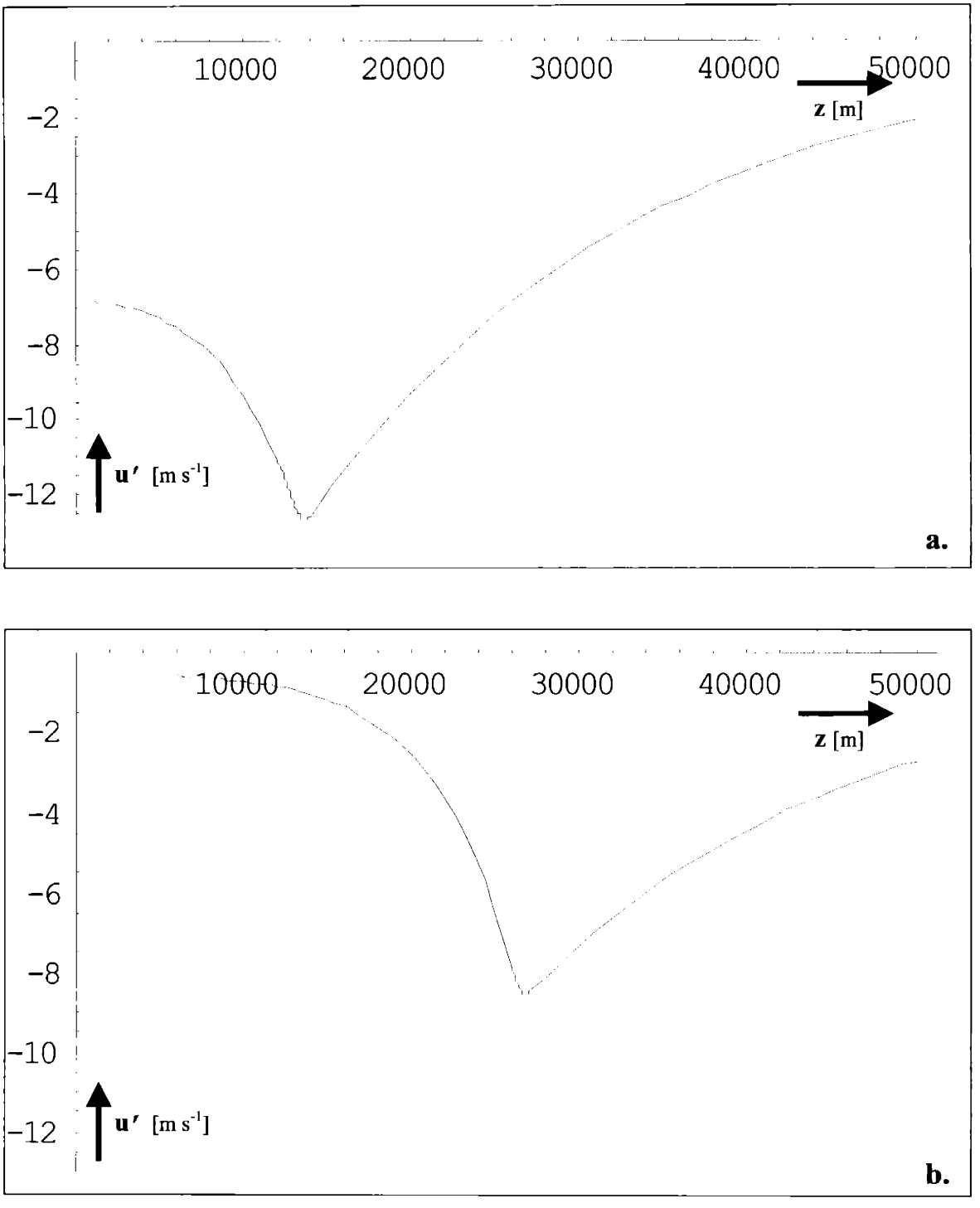

Figure 9. Zonal wind anomaly (u') height profile at $y = L/2$

a. 13 – 14 km Layer
b. 26 – 27 km Layer

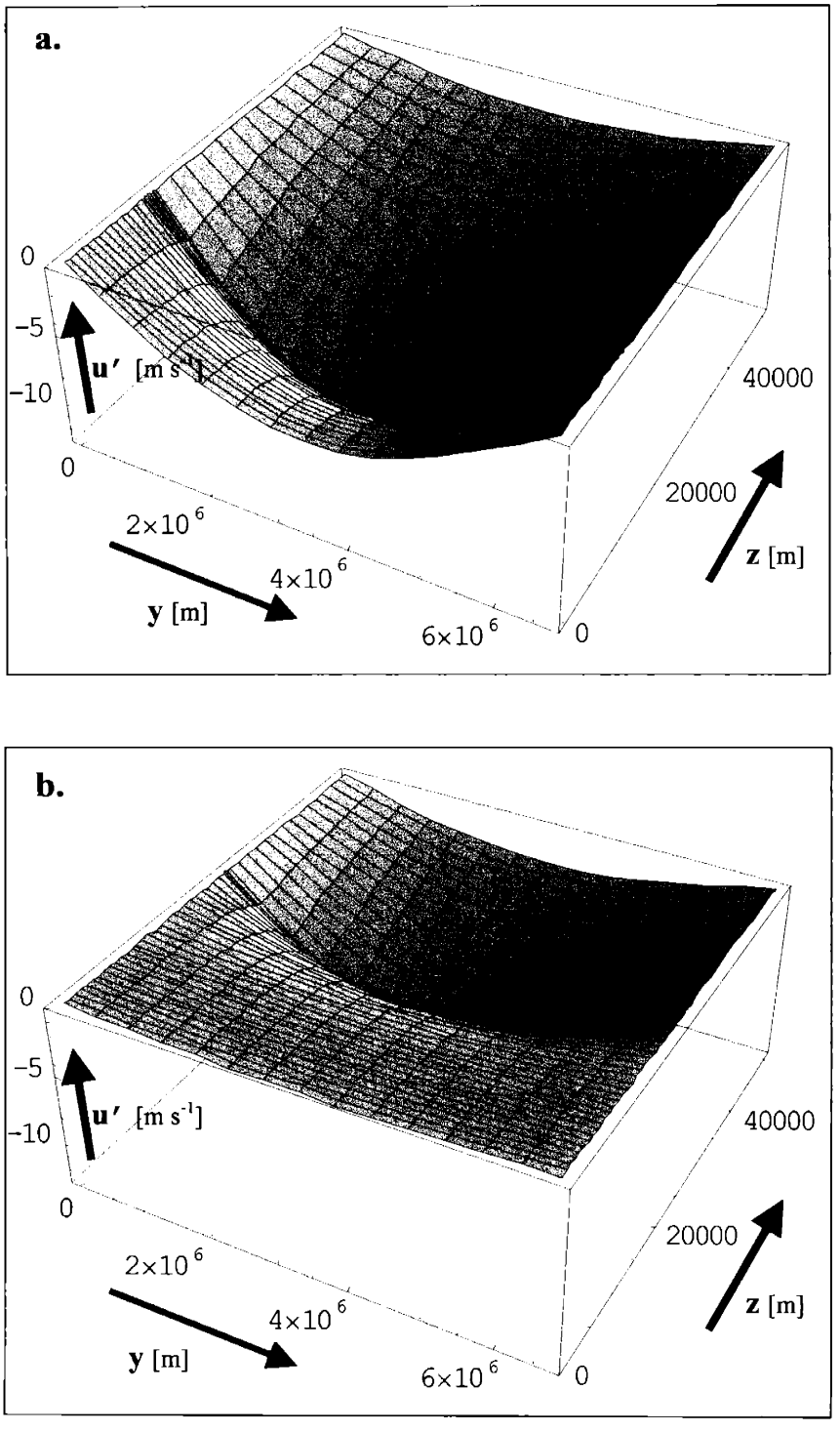

Figure 10. Zonal wind anomaly (u') field

a. 13 – 14 km Layer
b. 26 – 27 km Layer

From Figures 7-10, it is clear that the basic solution shapes remain unchanged as the height of the PV anomaly is moved upward in the stratosphere. While the geopotential height and zonal wind anomaly profiles possess the same basic shape structure, the temperature anomaly profile has a dissimilar shape by comparison. This may be attributed to the result of the subtraction performed in order to obtain the 13-14 km layer solution, i.e. the subtraction of the infinite layer above 14 km from that above 13 km, in combination with the approximate V-shape the infinite layer temperature anomaly profile possesses, as seen in Figure 4.

The major features in all of the solution plots, such as extreme points, change in altitude with the location of the PV anomaly layers. The geopotential height and zonal wind anomalies are always greatest at the midpoint in height of the PV anomaly layer, and then decay exponentially above and below with distance away from the height of the layer. This result is expected, since in the electrostatics analogy the non-local effect associated with an isolated localized electric charge decays with distance away from the source of the charge. Therefore, the associated non-local effect of the PV anomaly layer will always be greatest at the height of the PV layer, and will decay with distance away from that layer. The exponential decay may also be seen in the factors of $e^{[\ ]z}$ in the geopotential height anomaly solution given in Equation 9.

The values for the maximum geopotential height and zonal wind anomalies are greater in the solution for the lower layer than for the higher layer. This may be attributed to the fact that, although the thicknesses and PV anomaly magnitudes are equal for both layers, the mass of the lower layer is larger than the higher layer. Therefore, the

exponential decay with distance, combined with the fact that the upper layer also has a significantly smaller maximum zonal wind anomaly value compared to the lower layer, results in the magnitude of the zonal wind anomaly being significantly less at the surface in the case where the PV anomaly layer is located near the top of the lower stratosphere than in the case where it is by the tropopause, 0.51 m s^{-1} versus 6.8 m s^{-1}. In the real atmosphere, a zonal wind anomaly of approximately one meter per second at the surface is significant. Therefore, these results show that in terms of PV inversion, while the lower part of the lower stratosphere definitely has a significant signal at the surface of the earth, by comparison the surface signal associated with the top of the lower stratosphere is insignificant. This indicates that surface weather forecasting models which cap the simulated atmosphere at the tropopause most likely possess significant errors at the modeled surface. So while stratospheric dynamics must certainly be included in such models, the preceding PV inversion results indicate that simulation of the lower stratosphere alone may prove sufficient in representing the stratosphere as a whole when forecasting the weather at the surface of the earth. Though, it must be noted that the dynamics of the lower stratosphere may depend strongly on higher levels in the atmosphere in turn.

For a more detailed look at how the height in the stratosphere of a PV anomaly affects the associated surface signal, the surface zonal wind anomaly will be solved for for infinite layers above a variety of stratospheric heights. Table 2 gives the values of the surface zonal wind anomalies at $y = L/2$ for corresponding infinite layers of anomalous PV with constant value $Q = 1.0 \times 10^{-4}$ m^2 s^{-1} K kg^{-1} at different heights of H_{PV}.

H_{PV}	u_s' [m s^{-1}] at y = L/2
12.5 km	-41.9
13 km	-37.9
14 km	-31.1
15 km	-25.5
16 km	-20.8
17 km	-17.1
18 km	-14.0
19 km	-11.5
20 km	-9.38
21 km	-7.68
22 km	-6.29
23 km	-5.15
24 km	-4.22
25 km	-3.46
26 km	-2.83
27 km	-2.32
28 km	-1.90
29 km	-1.56
30 km	-1.27
35 km	-0.470
40 km	-0.173
45 km	-0.0638
50 km	-0.0235

Table 2. Constant PV Perturbation: u_s' for different H_{PV} heights

By adding and subtracting the solutions in Table 2, the value of the associated surface zonal wind anomaly can be determined for a realistic PV anomaly magnitude $Q = 1.0 \times 10^{-4}$ m^2 s^{-1} K kg^{-1} layer at any height in the stratosphere and of any thickness. It may be concluded that the higher the PV layer is in the stratosphere, the weaker its

associated surface signal. Also, the thicker the PV layer is, the greater its associated surface signal. This latter result may be attributed to the fact that as the thickness of the layer increases so does its volume. Since the value of the PV has been specified to be constant throughout the entire layer, as the layer grows in thickness, so does the overall magnitude of the PV anomaly and its associated surface signal.

The results in Table 2 confirm the conclusions made from Figures 7-10, that primarily only PV anomalies located in the lower stratosphere have significant associated surface signals, of O (1 m s^{-1}). Levels much above the lower stratosphere only possess insignificant or barely significant associated surface signals. Therefore, while surface weather forecasting models must include the stratospheric dynamics discussed above, it may be reasonable to limit the stratospheric simulation to the lower stratosphere alone in order to minimize computational costs.

V. TRANSIENT SOLUTION MODEL – Case 2

The next case examined in the transient solution model involves examining the effect that the level of wave dissipation in the stratosphere has on the weather at the surface of the earth. This study will be constructed as follows. The wave flux up from the solid surface of the earth will be held constant, while the level in the stratosphere above which the waves are assumed to completely dissipate is moved to varying heights. The magnitude of the PV anomaly in the infinite layer above H_{PV} will be calculated and then inverted to determine the related zonal wind anomaly field at the surface of the earth. Because the piecewise PV inversions are being performed under the assumption of QG, the

resulting solutions for the infinite PV anomaly layers may be unequivocally added and subtracted in order to determine how changing the height of wave dissipation in a finite layer in the stratosphere affects the magnitude of related change in the weather at the surface of the earth.

Wave propagation in the model will be represented by the Eliassen-Palm flux. It is defined as follows, noting that "[ ]" is used to indicate a zonally averaged quantity for completeness,

$$\vec{F} = \left(-\rho_R [u'v'], \frac{\rho_R f_0 [v'T']}{\frac{\partial T_R}{\partial z}} \right) = \left(F_y, F_z \right), \tag{10}$$

where ρ_R = reference density = $e^{-z/H_{S,T}}$. (10a)

The Eliassen-Palm flux is a particularly useful diagnostic tool because of the fact that it may be related to the flux of potential vorticity through the following equation,

$$[v'q_p'] = \frac{1}{\rho_R} \left(\nabla \cdot \vec{F} \right). \tag{11}$$

Rather than stating the magnitude of the constant surface wave flux explicitly, the surface wave flux may equivalently be represented by fixing the magnitude of a PV anomaly in a certain layer in the stratosphere. It will be assumed that the surface waves are solely vertically propagating and that these waves propagate up to an arbitrarily chosen level in the stratosphere at which they deposit all of their momentum, resulting in a certain magnitude PV anomaly in this layer. From this layer, the magnitude of the PV anomaly in any other selected stratospheric layer may then be calculated for the same constant wave flux as follows.

The inviscid, adiabatic, and zonally-averaged quasi-geostrophic PV equation is

$$\frac{\partial[q_p']}{\partial t} = -\frac{\partial}{\partial y}[v'q_p']. \tag{12}$$

Because it has been assumed that the waves are solely vertically propagating, then by Equation 11, the QG PV equation may be rewritten as

$$\frac{\partial[q_p']}{\partial t} = -\frac{\partial}{\partial y}\left(\frac{1}{\rho_R}\frac{\partial F_z}{\partial z}\right). \tag{13}$$

In an arbitrary layer between z_{01} and z_{02} in the stratosphere, q_{p0}' will be set to have a constant value with height, Q_0, corresponding to the maximum PV redistribution possible for a realistic magnitude surface wave flux. Then, since it is assumed that F_z is a fixed constant at the surface, in the instantaneous case of the transient solution the following definite integral may be solved for from Equation 13,

$$\int_{z_{01}}^{z_{02}} \rho q_{p0}'\, dz = \int_{z_{01}}^{z_{02}} \left(e^{-z/H_S}\right)\left(Q_0 \cos\frac{m\pi y}{L}\right) dz = C_0 \cos\frac{m\pi y}{L}, \tag{14}$$

where C_0 = constant.

Now the PV anomaly magnitude, Q_{ab}, for any selected stratospheric layer between z_a and z_b may be calculated as follows.

$$\int_{z_a}^{z_b} \rho q_{p\,ab}'\, dz = C_0 \cos\frac{m\pi y}{L}, \tag{15}$$

$$\text{so} \qquad \int_{z_a}^{z_b} Q_{ab}\left(e^{-z/H_S}\right) dz = C_0. \tag{16}$$

Once the PV anomaly magnitudes have been calculated for each of the layers of interest, piecewise PV inversion may be employed in order to determine the associated anomalous zonal wind and temperature fields throughout the height of the atmosphere for each layer.

In this study, it is of greatest interest to examine how the magnitude of the zonal wind anomaly at the surface changes for different corresponding stratospheric PV layers. Here, a PV anomaly with magnitude $Q_0 = 1.0 \times 10^{-4}$ m^2 s^{-1} K kg^{-1} will arbitrarily be imposed in a layer between 13 - 14 km, with all other layers calculated from this. Presented in Table 3 are the values of surface zonal wind anomalies at $y = L/2$ calculated from PV anomalies determined for equal one kilometer thickness layers chosen throughout the height of the stratosphere.

Layer (z_a - z_b)	**Q_{ab}' [m^2 s^{-1} K kg^{-1}]**	**u_s' [m s^{-1}] at y = L/2**
13 – 14 km	1.00×10^{-4}	-6.87
14 – 15 km	1.16×10^{-4}	-6.53
15 – 16 km	1.35×10^{-4}	-6.21
16 – 17 km	1.57×10^{-4}	-5.91
17 – 18 km	1.82×10^{-4}	-5.62
18 – 19 km	2.11×10^{-4}	-5.34
19 – 20 km	2.45×10^{-4}	-5.08
20 – 21 km	2.85×10^{-4}	-4.83
21 – 22 km	3.31×10^{-4}	-4.60
22 – 23 km	3.84×10^{-4}	-4.37
23 – 24 km	4.46×10^{-4}	-4.16
24 – 25 km	5.18×10^{-4}	-3.96
25 – 26 km	6.01×10^{-4}	-3.76
26 – 27 km	6.98×10^{-4}	-3.58
27 – 28 km	8.11×10^{-4}	-3.40
28 – 29 km	9.41×10^{-4}	-3.24
29 – 30 km	1.09×10^{-3}	-3.08
30 – 31 km	1.27×10^{-3}	-2.92
31 – 32 km	1.47×10^{-3}	-2.78
32 – 33 km	1.71×10^{-3}	-2.65
33 – 34 km	1.99×10^{-3}	-2.52
34 – 35 km	2.31×10^{-3}	-2.40
35 – 36 km	2.68×10^{-3}	-2.28
36 – 37 km	3.11×10^{-3}	-2.17
37 – 38 km	3.61×10^{-3}	-2.06

38 – 39 km	4.20×10^{-3}	-1.96
39 – 40 km	4.87×10^{-3}	-1.86
40 – 41 km	5.66×10^{-3}	-1.77
41 – 42 km	6.57×10^{-3}	-1.69
42 – 43 km	7.63×10^{-3}	-1.60
43 – 44 km	8.86×10^{-3}	-1.53
44 – 45 km	1.03×10^{-2}	-1.45
45 – 46 km	1.19×10^{-2}	-1.37
46 – 47 km	1.39×10^{-2}	-1.31
47 – 48 km	1.61×10^{-2}	-1.25
48 – 49 km	1.87×10^{-2}	-1.19
49 – 50 km	2.17×10^{-2}	-1.13
50 – 51 km	2.52×10^{-2}	-1.07
51 – 52 km	2.93×10^{-2}	-1.02
52 – 53 km	3.40×10^{-2}	-0.971
53 – 54 km	3.95×10^{-2}	-0.924

Table 3. Constant Surface Wave Flux: u_s' for different q_p' heights

It should again be noted that QG only holds up to an approximate height of 30 km, although it is still nonetheless interesting to examine the results above 30 km. The surface zonal wind anomalies are all of O (1 m s^{-1}), and may therefore be considered to be of a significant magnitude at the surface of the earth. Cursory examination of the above results also reveals that for a constant surface wave flux, the magnitude of the PV anomaly increases exponentially as the height of the layer rises in the stratosphere, while the surface zonal wind anomaly experiences an exponential decrease in magnitude. This may be seen more clearly in the following plots of $ln\ Q_{ab}$ and u_s' against the height of the lower boundary of the one kilometer layers, z_a, in Figures 11 and 12 respectively, taken from Table 3.

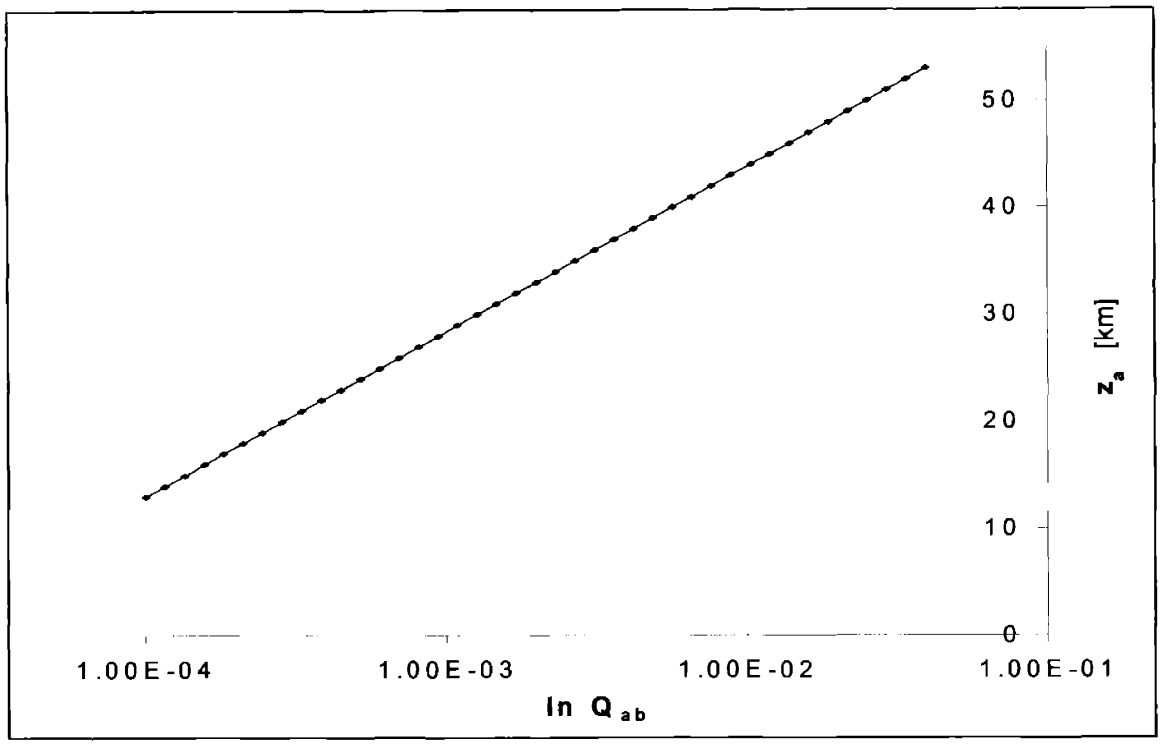

Figure 11. Table 3 Data – Plot 1: ln Q_{ab} vs. z_a

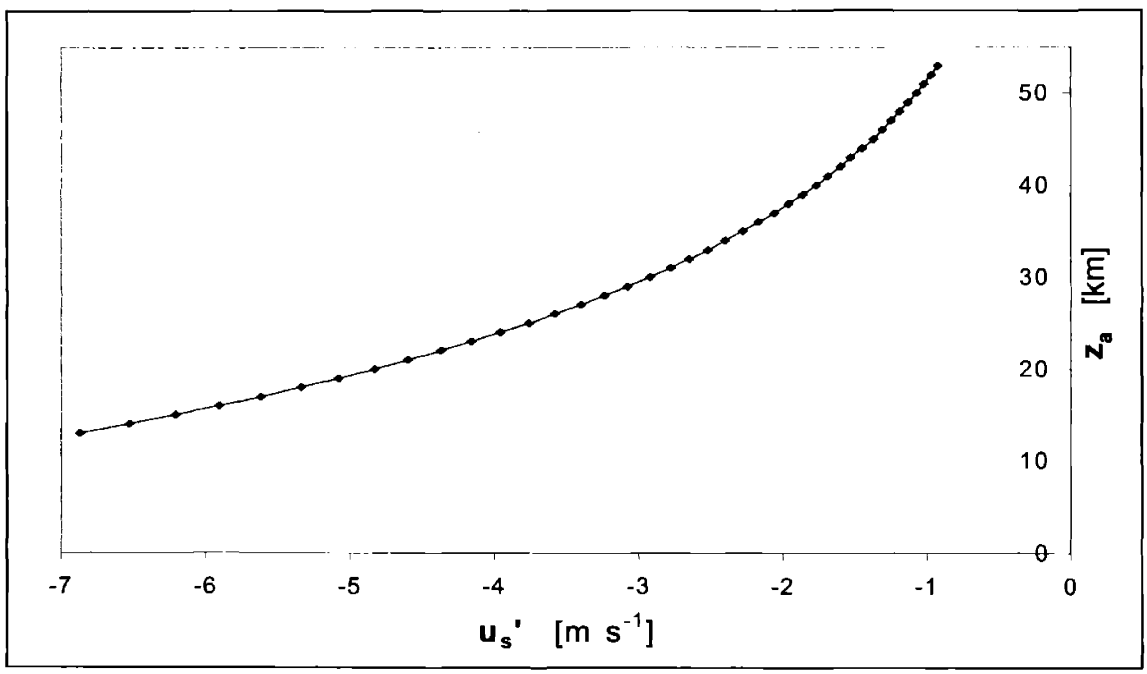

Figure 12. Table 3 Data - Plot 2: u_s' vs. z_a

Though the PV perturbation grows in magnitude as the layer is raised, it is not enough to offset the weakening of the magnitude of the surface signal due to the subsequently increased depth of atmosphere that the signal must pass through. Overall, the higher the surface waves break in the stratosphere, the weaker the corresponding surface signal is in terms of zonal wind. PV inversion in general does not allow for a determination of cause and effect, it only allows for a determination of association. However, the particular construction of this transient case of a constant surface wave flux breaking at different stratospheric levels does allow for the determination that the stratosphere has a significant impact on surface weather, since the flux of waves up from the solid surface of the earth remains fixed and only the height at which these waves break in the stratosphere is changing. In other words, if the stratospheric dynamics described above were to be excluded from models attempting to simulate the weather at the surface of the earth, the resulting simulations would be in significant error.

In order to try and further understand the dynamics behind the exponential decrease in the surface zonal wind anomaly for a constant surface wave flux breaking at subsequently higher levels in the stratosphere, the relevant equations will now be examined. In this way, an attempt may be made to try to determine the relative importance each involved atmospheric parameter has in influencing the above observed dynamics. The relationship between the following two arbitrary layers in the stratosphere will be examined: a lower layer subscripted L bounded below by z_1 and above by z_2, and an upper layer subscripted U and bounded below by z_3 and above by z_4. It is useful to think of the lower layer as the previously described control-case layer with a fixed constant PV

anomaly magnitude, Q_0, in order to make the dynamical analyses more comprehensible, as this was the model setup used for the results given in Table 3. For simplification, it will be assumed that the layers are of equal thickness, i.e. that $z_2 - z_1 = z_4 - z_3$. A relationship between the magnitudes of the PV anomalies in the two layers follows,

$$q_{pU}' = \left(e^{\frac{z_3 - z_1}{H_S}} \right) * q_{pL}'. \tag{17}$$

This accounts for the observed exponential increase in the magnitude of the PV anomaly with height, since $z_3 - z_1$ increases as the upper layer is moved further away from the lower layer. The following relationship may be given for the surface zonal wind anomaly associated with the upper layer,

$$u_{sU}' = K\, q_{pU}' \left(e^{-b z_3} - e^{-b z_4} \right), \tag{18}$$

where

$$K = -\frac{L}{\pi} \left[\frac{\left(1 - \frac{d}{c}\right) a c e^{b H_{TR}}}{c d \left(e^{c H_{TR}} - e^{d H_{TR}} \right) + a \left(c e^{d H_{TR}} - d e^{c H_{TR}} \right)} \right] = \text{constant}, \tag{18a}$$

and a, b, c, and d are given by Equations 9a and 9b. By applying Equation 17 to Equation 18, a relationship may also be obtained between u_{sU}' and q_{pL}'. Examining Equation 18 reveals that as the upper layer is moved away from the lower layer, the surface zonal wind anomaly experiences exponential growth from the magnitude of the PV anomaly as mentioned above, but exponential decay as a result of the $\left(e^{-b z_3} - e^{-b z_4} \right)$ term which decreases in value as z_3 and z_4 increase. The product of these two terms, however, ultimately results in an overall exponential decrease in the magnitude of the surface zonal

wind anomaly as the upper layer is moved upward in the stratosphere. This may be seen by examining Equation 9a more closely. The characteristic length-scale of midlatitudes, or Rossby radius of deformation, is $L_R = \frac{NH}{f_0}$. For $L \approx L_R$, Equation 9a may be approximated as $b \approx \left(\frac{1+\sqrt{5}}{2}\right) * \frac{1}{H_S}$. Therefore, as long as the chosen length-scale L is approximately equal to the characteristic length-scale of midlatitudes, b will always be greater than $\frac{1}{H_S}$. Consequently, the magnitude of the surface zonal wind anomaly in this case will always decrease as the height of the resultant PV layer is moved upwards in the stratosphere.

The scale height in the stratosphere, H_S, plays an important role in determining the rate at which the magnitude of the surface zonal wind anomaly decreases as the upper layer is further removed. For example, the rate of decrease of the surface zonal wind anomaly is significantly slower using the scale height value for the troposphere. This means that at the tropopause and above, the rate of decrease in magnitude of the surface zonal wind anomaly will significantly increase. This is primarily a result of the fact that the stratosphere has a significantly smaller mass than the troposphere, meaning that this fact does play an important role in the dynamics between the stratosphere and its associated effect at the surface of the earth. Although the rate of decrease in anomalous surface zonal wind increases rapidly in the stratosphere as compared to in the troposphere, the calculated values given in Table 3 show that the associated surface zonal wind anomalies are nonetheless still significant. However, it does mean that it is the lower-most part of the

stratosphere that has the greatest associated effect at the surface of the earth, as may clearly be seen in Figure 12.

It may be concluded from this study that the stratosphere has a significant associated effect at the surface of the earth for a constant flux of waves up from the surface under the method of piecewise PV inversion. Therefore, the dynamics of this relationship must be included in any models of surface weather. The results of this study indicate that, due to the small mass of the stratosphere and the dynamics of the stratosphere-surface link, it is primarily the lowest part of the stratosphere that has the most significant impact on the weather at the surface. This confirms the deduction made in the previous section that, for a constant value PV anomaly moved to different heights in the stratosphere, it was only the lower stratosphere that had a significant impact at the surface of the earth. Consequently, both transient solution model studies performed here indicate that while stratospheric simulation is necessary when forecasting the weather at the surface of the earth, it may reasonably be limited to the lower stratosphere alone with minimal loss in skill if using the method of piecewise PV inversion.

VI. STATIONARY SOLUTION MODEL

While the transient solution model enabled the link between the stratosphere and the surface of the earth to be examined on short time scales in order to assess the effect of the stratosphere on surface weather, the stationary solution model presented here will allow this link to be examined in the time-averaged state instead in order to provide a steady-state picture of how the stratosphere influences climate at the surface of the earth. The

method of piecewise PV inversion under the assumption of QG will also be used to diagnose the stratosphere-troposphere link here in the stationary solution model.

Like the transient solution model, the stationary solution model will be set up using log-pressure height coordinates on a beta-plane in a rigid channel of width L under the assumption of QG and assuming that there are no variations in the zonal direction. However, because of the long time-scale of the stationary solution, the adiabatic and inviscid assumptions that were made in the transient solution model will not be made here. Instead, heating will be represented by Newtonian cooling,

$$Q = \textit{diabatic heating} = \frac{T_E - T}{\tau_E}, \tag{19}$$

where T_E = in a state of convective-radiative equilibrium, (19a)

and τ_E = radiative time-scale = 30 days = 2.6 x 10^6 s. (19b)

While friction will still be assumed to be zero in the atmosphere, it will now be assumed to be non-zero at the surface. Surface drag only becomes significant here in steady-state because it is generally of a small enough magnitude that on the short time-scales of the transient solution it may be ignored. The assumption of steady-state,

$$\frac{\partial}{\partial t} = 0, \tag{20}$$

will also be made.

Similar to the second study done in the transient solution model, a constant surface wave flux will be induced to the system initially at rest, and the level at which these waves are selected to dissipate will be changed. In this case, the surface wave flux will be stated explicitly via the Eliassen-Palm flux, noting that the Eliassen-Palm flux is equally valid in

both the transient and stationary solutions. It will be assumed that the surface waves are solely vertically propagating, i.e. $F_y = 0$, and that these waves are the only source of wave activity in the system, with the vertical component of the Eliassen-Palm flux as follows,

$$F_z = \int_z^\infty \rho_R [v' q_p'] dz . \tag{21}$$

This means that the net wave drag in the vertical column of the atmosphere above the source of the wave flux is equal to the wave drag at the surface, i.e. the only source of momentum in the system comes from the surface stress, τ_s. This may be written as,

$$\int_0^\infty \rho_s [v' q_p'] dz = -\tau_s . \tag{22}$$

The surface stress may in turn be related to the surface zonal wind anomaly as follows,

$$\tau_s = \rho_s c_D |u_s'| u_s', \tag{23}$$

where

ρ_s = surface density = 1.225 kg m^{-3}, and (23a)

c_D = drag coefficient = 2 x 10^{-3}. (23b)

The poleward flux of potential vorticity, $[v' q_p']$, will be specified as well. In order to emulate the true steady-state atmosphere, the PV poleward flux will be assumed to vary latitudinally as a modal sine function and to vary in height by some arbitrary function that is assumed to decay to zero as $z \rightarrow \infty$. The equation follows,

$$[v' q_p'] = Z(z) \sin \frac{m \pi y}{L} . \tag{24}$$

As in the transient model solution, summing the solutions of Equation 24 for selected different modal values, m, will allow the construction of any shape for the poleward PV flux. For simplicity, it will be assumed that m = 1 here. Equations 22-24 may be

combined to give the following equation relating the surface zonal wind to the constant vertical component of the Eliassen-Palm flux at the surface, F_s,

$$|u_s'|u_s' = -\frac{1}{\rho_s c_D} F_s \sin\frac{m\pi y}{L}, \tag{25}$$

where

$$F_s = -\int_0^\infty \rho_s Z(z)\, dz = f(z)\big|_{z=0} = \text{ fixed constant.} \tag{26}$$

In the transient solution model, the strength of the surface signal for different PV heights was assessed by measuring the corresponding changes in value of the associated zonal wind anomalies at the surface. However, in the stationary solution, the value of the surface zonal wind remains fixed regardless of the height in the stratosphere at which the surface waves dissipate, as seen in Equation 25. Therefore, the stationary solution model study will be executed in the reverse order of the method used in the transient solution model. Instead of inverting the changing stratospheric PV to give the associated surface zonal wind anomaly value as in the transient case, this study will begin with the value of the steady-state perturbation zonal wind at the surface and from this, obtain the stratospheric PV. Then, it may be examined how the magnitude and height profile of the PV anomaly changes as the level of wave dissipation varies, while still always giving the same associated steady-state magnitude of anomalous zonal wind at the surface. This will be the method used to examine the relationship between the stratosphere and the surface in the stationary case.

The PV anomaly profile in the atmosphere will be determined by solving for the perturbation zonal wind, then integrating this solution in Equation 2 to solve for the geopotential height anomaly, and finally using the solution for ψ' in Equation 3 to obtain

the solution for q_p'. The anomalous zonal wind solution will be determined using the set of equations given below.

Transformed Eulerian Mean (TEM) Momentum Equation:

$$\frac{\partial [u']}{\partial t} - f_0 [v]_R = \frac{1}{\rho_R}\left(\nabla \cdot \vec{F}\right) + [\mathcal{F}_1] \tag{27}$$

Transformed Eulerian Mean (TEM) Thermodynamic Equation:

$$\frac{\partial [T']}{\partial t} + \frac{T_{S,T} N_{S,T}^{\ 2}}{g} [w]_R = [\mathrm{Q}] \tag{28}$$

Transformed Eulerian Mean (TEM) Equation of Continuity:

$$\frac{\partial [v]_R}{\partial y} + \frac{1}{\rho_R}\frac{\partial}{\partial z}\left(\rho_R [w]_R\right) = 0 \tag{29}$$

Thermal Wind Equation:

$$f_0 \frac{\partial [u']}{\partial z} = -\frac{g}{T_{S,T}} \frac{\partial [T']}{\partial y} \tag{30}$$

where the residual wind is defined by

$$[v]_R = [v] - \frac{1}{\rho_R}\frac{\partial}{\partial z}\left(\rho_R \frac{[v'T']}{\left(\frac{\partial T_{S,T}}{\partial z}\right)}\right), \text{ and}$$

$$[w]_R = [w] + \frac{\partial}{\partial y}\left(\frac{[v'T']}{\left(\frac{\partial T_{S,T}}{\partial z}\right)}\right),$$

and where $[\mathcal{F}_1]$ = x-component of acceleration due to friction = 0, and

$T_{S,T}$ and $N_{S,T}$ are as defined in Table 1.

Applying the steady-state assumption (Equation 20) and the chosen function for the poleward PV flux (Equation 24) to the TEM momentum equation (Equation 27), allows the residual wind $[v]_R$ to be solved for,

$$[v]_R = -\frac{1}{f_0} Z(z) \sin\frac{m\pi y}{L}. \tag{31}$$

Using this equation for $[v]_R$ in the TEM equation of continuity (Equation 29) gives the following equation for $[w]_R$,

$$[w]_R = \left(\frac{m\pi}{\rho_R f_0 L}\right) \int_z^\infty \rho_R Z(z)\, dz \left(\cos\frac{m\pi y}{L}\right). \tag{32}$$

Applying this solution of $[w]_R$ to the TEM thermodynamic equation (Equation 28) gives the perturbation temperature solution,

$$[T'] = -\left(\frac{T_{S,T}\, \tau_E\, N_{S,T}{}^2}{\rho_R f_0\, g} \frac{m\pi}{L}\right) \int_z^\infty \rho_R Z(z)\, dz \left(\cos\frac{m\pi y}{L}\right), \tag{33}$$

Finally, the solution for $[T']$ will be used in the thermal wind equation (Equation 30) to obtain the zonal wind anomaly shear with height,

$$\frac{\partial[u']}{\partial z} = -\left(\frac{K_{S,T}}{\rho_R}\right) \int_z^\infty \rho_R Z(z)\, dz \left(\sin\frac{m\pi y}{L}\right), \tag{34}$$

$$\text{where} \quad K_{S,T} = \left(\frac{\tau_E N_{S,T}{}^2}{f_0{}^2} \frac{m^2\pi^2}{L^2}\right) = \text{constant}. \tag{34a}$$

With the above solutions in hand, the stationary solution model will proceed to be constructed as follows. The constant surface wave flux, depicted by

$$F_z\big|_{z=0} = F_s \sin\frac{m\pi y}{L}, \tag{35}$$

where F_s is given by Equation 26, is assumed to propagate up into the stratosphere to some level where it is assumed the waves entirely dissipate in an atmospheric layer of finite thickness. The layer of dissipation will arbitrarily be specified to be bounded above and below in the stratosphere by z_a and z_b respectively. The waves are assumed to experience no dissipation before they reach the level of dissipation, and so F_z will possess the value of F_s up to the lower boundary of the dissipation layer. Because the waves are assumed to entirely dissipate within the specified stratospheric layer, the value of F_z will then decrease from a value of F_s at the bottom of the layer to zero at the top of the layer, and will be identically zero throughout the rest of the atmosphere upwards to infinity. Due to the distinct values of $T_{S,T}$, $H_{S,T}$, and $N_{S,T}$ in the stratosphere and troposphere, the atmosphere in the stationary solution model will be split into the following four sections as depicted in Figure 13.

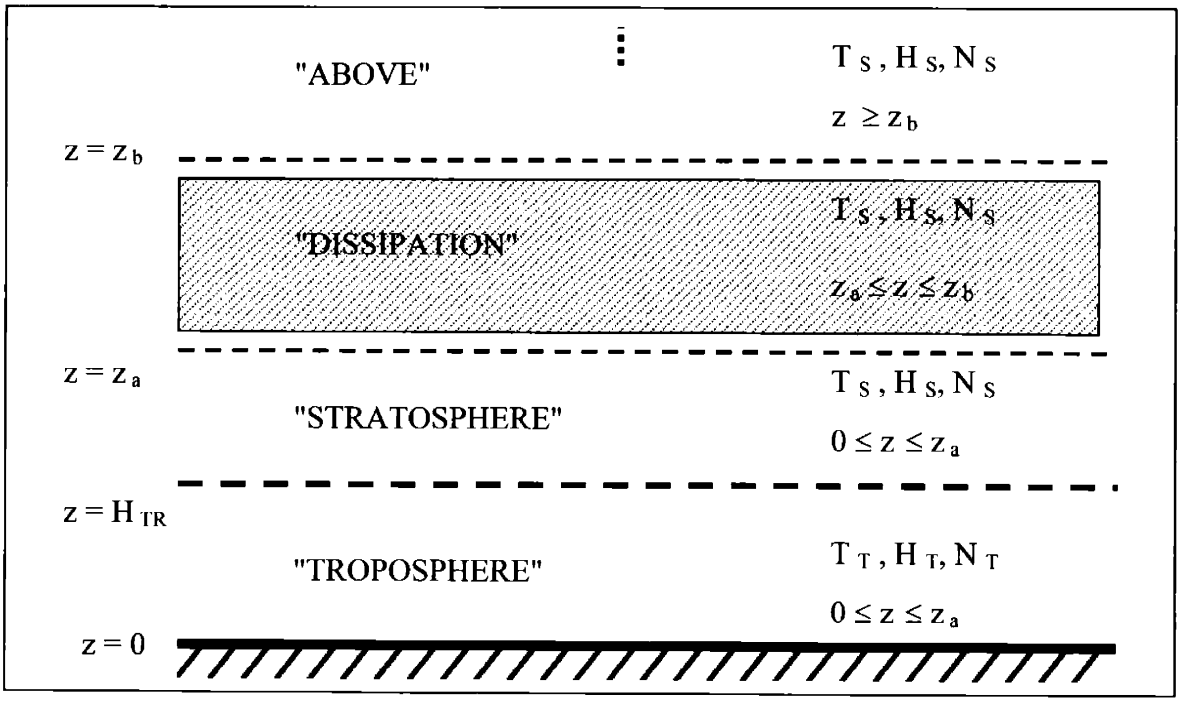

Figure 13. Stationary solution model setup

The structure of the vertical component of the Eliassen-Palm flux (Equation 21) is determined by the structure of the poleward PV anomaly flux (Equation 24). Therefore, in order to construct F_z so that it has the profile described above, for simplicity the product of the reference density with the variation of $[v'q_p']$ with height will be specified to be constant throughout the layer of dissipation and zero everywhere else, as follows,

$$\rho_R Z(z) = \begin{cases} 0 & for \quad z \geq z_b \\ C = \text{constant} & for \quad z_a \leq z \leq z_b \\ 0 & for \quad 0 \leq z \leq z_a \end{cases}. \tag{36}$$

Note that by applying the above Equation 36 to Equation 26, the constant C may be solved for from the following relation to the calculated fixed constant surface wave flux F_s,

$$C = \frac{F_s}{z_b - z_a}. \tag{37}$$

Therefore, the vertical component of the Eliassen-Palm flux now has the following profile in the atmosphere,

$$F_z = \left(\sin\frac{m\pi y}{L}\right) * \begin{cases} 0 & for \quad z \geq z_b \\ C(z_b - z) & for \quad z_a \leq z \leq z_b \\ F_s & for \quad 0 \leq z \leq z_a \end{cases}. \tag{38}$$

The zonal wind shear from Equation 34 may now be written

$$\frac{\partial [u]'}{\partial z} = \left(\sin \frac{m\pi y}{L} \right) * \begin{cases} 0 & for \quad z \geq z_b \\ -\dfrac{KC}{\rho_R}(z_b - z) & for \quad z_a \leq z \leq z_b \\ -\dfrac{K}{\rho_R} F_s & for \quad 0 \leq z \leq z_a \end{cases} . \tag{39}$$

Note that the above solutions all contain a sinusoidal function in y. Therefore, the solutions may be written as being comprised of distinct functions in y and z as follows,

$$h(y,z) = f(z)\, g(y),$$

where it is assumed that all constants are absorbed into the function $f(z)$, and so

$$g(y) = \sin, \cos \left(\frac{m\pi y}{L} \right).$$

The primary focus of the study here is to examine how the PV magnitude and profile changes as the dissipation height of the surface waves is moved. Because the longitudinal variations in the solutions, represented by $g(y)$, do not change as the height of wave dissipation is moved through the stratosphere, writing the solutions in this separable form allows the changes in variation with height, in $f(z)$, to be more easily assessed. Therefore, the solution for the perturbation zonal wind may be written as,

$$u'(y,z) = U'(z) \left(\sin \frac{m\pi y}{L} \right) \tag{40}$$

Substituting this into Equation 2 and integrating yields the following general solution for the perturbation geopotential height,

$$\psi'(y,z) = \frac{L}{m\pi} U'(z) \left(\cos \frac{m\pi y}{L} \right) \tag{41}$$

The geopotential height may now be used in Equation 3 in order to obtain the solution for the PV perturbation field. In solving for q_p', the computation of the partial derivatives with respect to y and z is relatively straightforward, with the derivatives with respect to z determined directly from the equation for the zonal wind shear (Equation 39). After simplification, the equation for PV may be written as follows,

$$q_p'(y,z) = \left(\cos\frac{m\pi y}{L}\right) * \begin{cases} -\frac{m\pi}{L}U'(z) & for \quad z \geq z_b \\ \frac{m\pi}{L}\left(\frac{\tau_E}{\rho_R}C - U'(z)\right) & for \quad z_a \leq z \leq z_b \\ -\frac{m\pi}{L}U'(z) & for \quad 0 \leq z \leq z_a \end{cases} \qquad (42)$$

$$= q_p'(z)\left(\cos\frac{m\pi y}{L}\right)$$

The constant value of $U'(0)$ may be determined from Equation 25. The zonal wind height profile may then be constructed by integrating upward from this surface value using the equation for zonal wind shear (Equation 39). This completes the general solution for q_p' in the stationary solution model.

The magnitude of the surface zonal wind and consequently the height profiles of the zonal wind and PV are dependent upon the magnitude of the surface wave flux. The constant value for the surface wave flux will be calculated from Equation 10 using typical Northern hemispheric surface steady-state atmospheric values as follows,

$$F_s = \frac{\rho_R f_0 [v'T']}{\left(\frac{\partial T_R}{\partial z}\right)} = \frac{\left(1.225\ \text{kg m}^{-3}\right)\left(10^{-4}\ \text{s}^{-1}\right)\left(2\ \text{K m s}^{-1}\right)}{\left(2.5 \times 10^{-3}\ \text{K m}^{-1}\right)} = 9.8 \times 10^{-2}\ \text{kg m}^{-1}\ \text{s}^{-2}, \qquad (43)$$

where the value for the stationary poleward flux of PV was obtained from Figure 13.5 in Peixoto and Oort [1992]. Using this value for F_s gives the following plot for the fixed surface zonal wind.

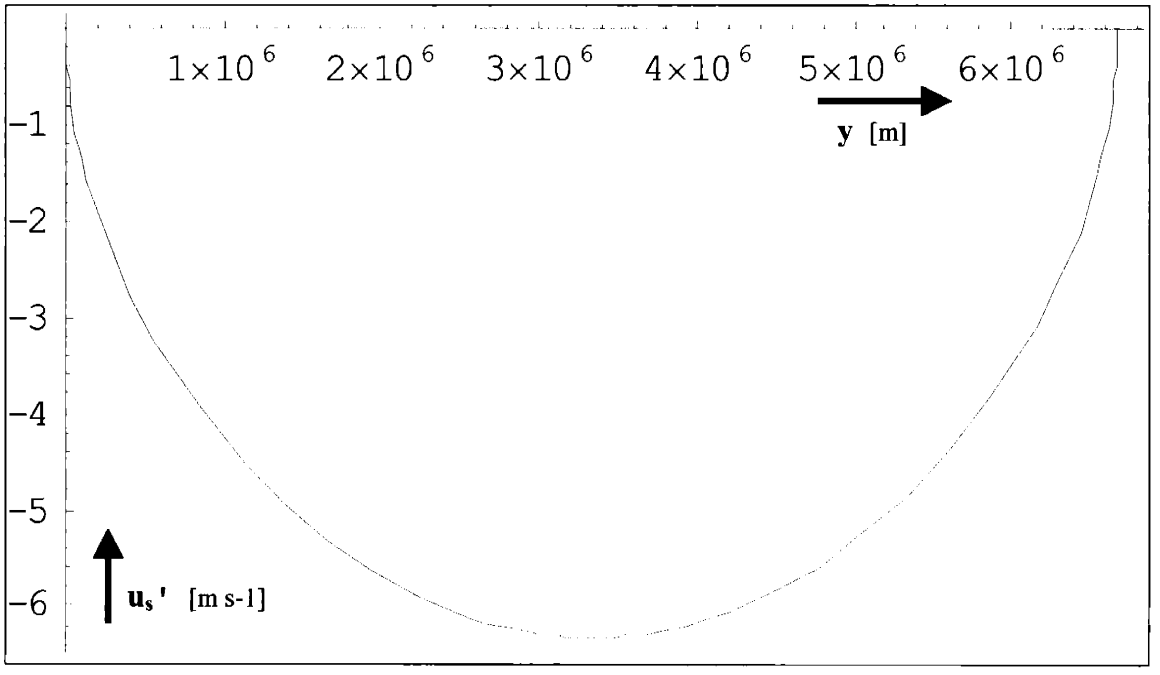

Figure 14. Surface zonal wind anomaly (u_s') plot

The maximum value of the perturbation surface zonal wind is

$$u_s'\,(y = L/2) = U'(z = 0) = -\,6.32\ \text{m s}^{-1}. \tag{44}$$

Thus, in the stationary case a reasonable eddy flux of topographically forced surface waves results in a significant signal at the surface in perturbation zonal wind.

As mentioned earlier, because the zonal wind at the surface is determined solely by the value of the constant surface wave flux, it also remains fixed regardless of where in the atmosphere the surface waves ultimately end up dissipating. This is unlike what took place in the transient solution, where the value of the surface zonal wind anomaly did change depending upon the height of wave dissipation. The reason behind this discrepancy has to

do with the difference in time-scales between the transient and stationary solutions. In the transient case, the time-scale is of the order of days. Thus, the effect of surface friction is rendered insignificant in comparison to the large dominating turbulent motions present in the transient model atmosphere. On the other hand, in the stationary solution only time-averaged motions are present in the model atmosphere. Therefore, the short time-scale atmospheric motions that dominated in the transient case are no longer present in the stationary case, having been averaged out. This allows surface friction to be an important factor in the stationary solution, and in fact the only factor in determining the steady-state perturbation surface zonal wind.

Now, with the fixed solution of the perturbation zonal wind at the surface, given in Figure 14, the stationary solution model may be run for varying dissipation layer thicknesses and heights, in order to see what effect changing the dissipation layer has on the PV and zonal wind anomaly height profiles. From this, it may then be determined how the PV anomaly profile is linked to the surface zonal wind anomaly solution. Hopefully this will, as a result, allow additional insight to be gained into the dynamics between the stratosphere and the surface.

In order to compare the effect of the height of the dissipation layer in the stratosphere on the PV and zonal wind anomaly profiles, the stationary solution model will be run for a layer located by the tropopause between 13-14 km, and another layer of the same thickness located between 26-27 km at the top of the lower stratosphere. To then assess the effect the thickness of the dissipation layer has, the model will be run a third time for a layer between 13-15 km, at approximately the same height and twice the

thickness of the 13-14 km layer. Note that the choice of layers is arbitrary and the model may be run for any combination of layer thickness and height just as easily as for those chosen here, limited only by the constraint that the layers be located in the stratosphere. The zonal wind and PV anomaly profiles for the selected layers will be presented here for comparison. The values for the constants used in the stationary solution model runs may be determined from Table 1, and Equations 19b, 23a b, 37, and 43.

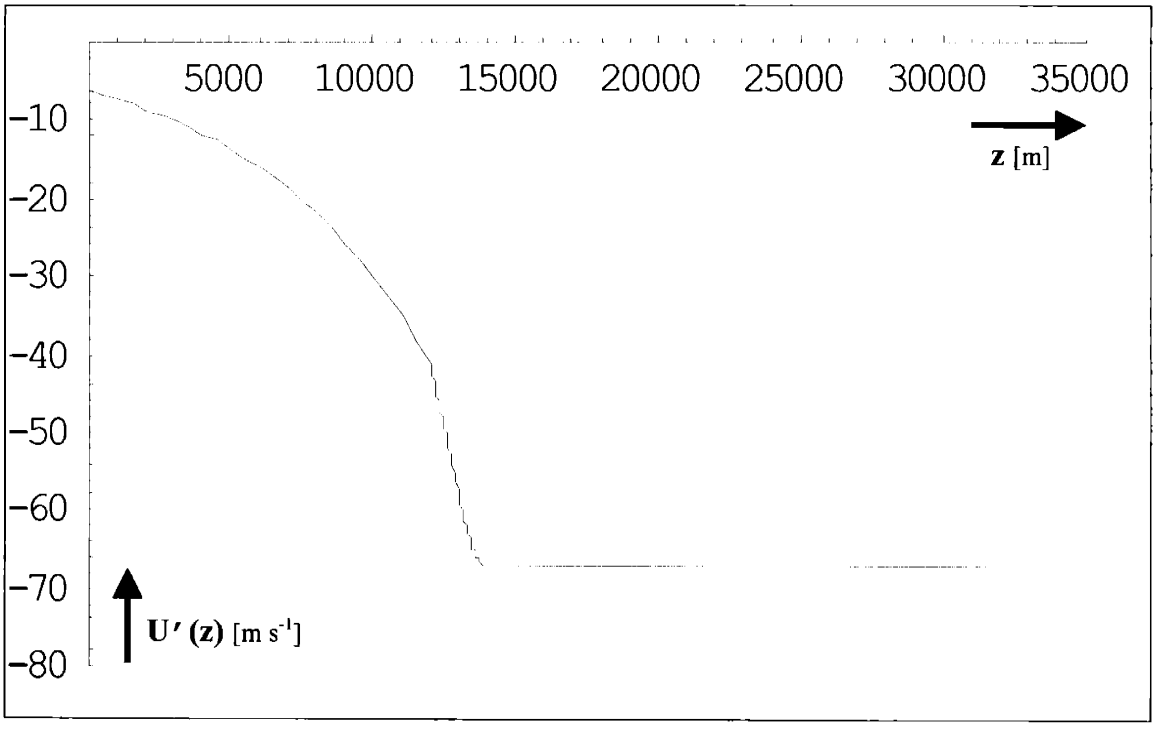

Figure 15. Zonal wind anomaly height profile ($U'(z)$) for 13-14 km layer

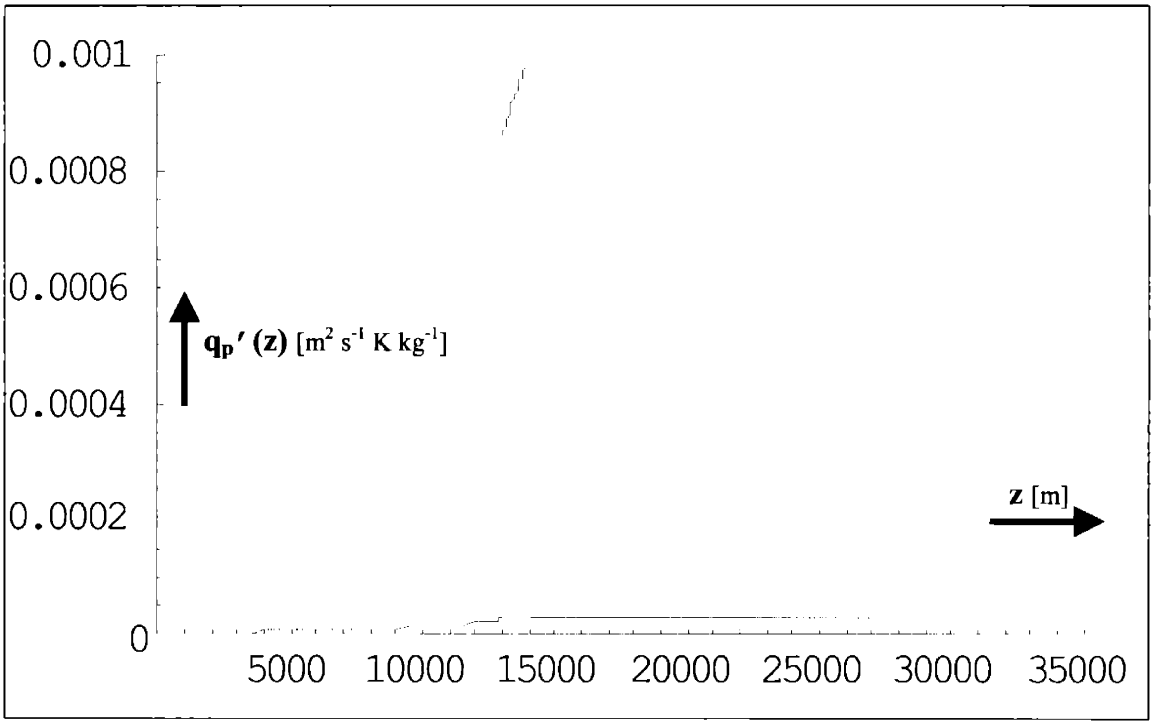

Figure 16. PV anomaly height profile ($q_p'(z)$) for 13-14 km layer

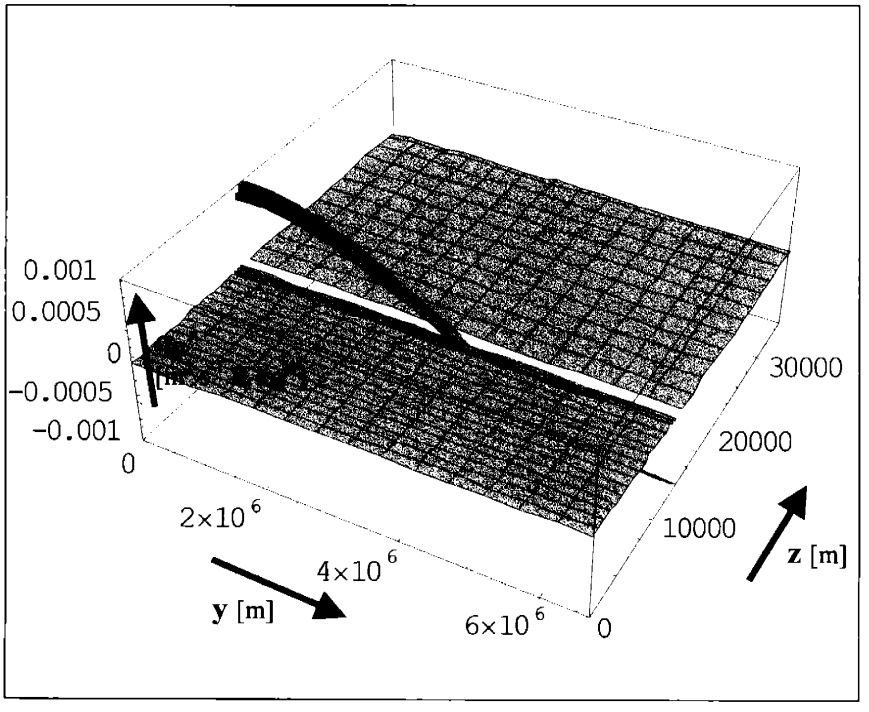

Figure 17. PV anomaly field (q_p') for 13-14 km layer

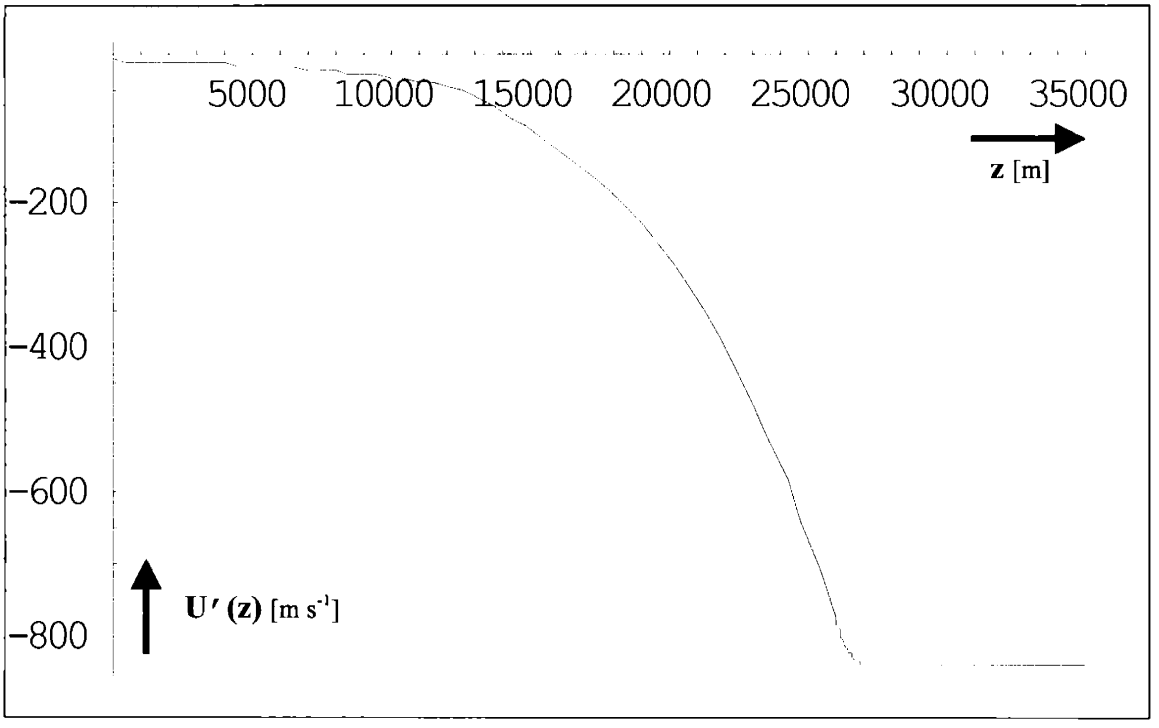

Figure 18. Zonal wind anomaly height profile ($U'(z)$) for 26-27 km layer

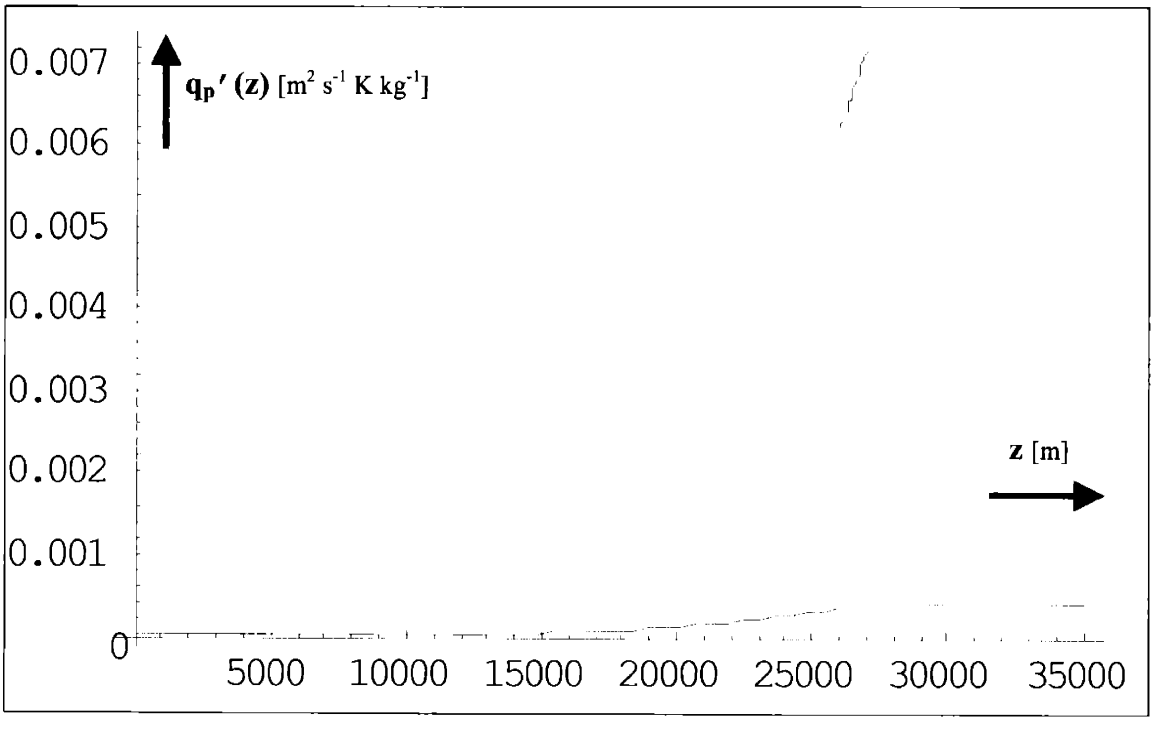

Figure 19. PV anomaly height profile ($q_p'(z)$) for 26-27 km layer

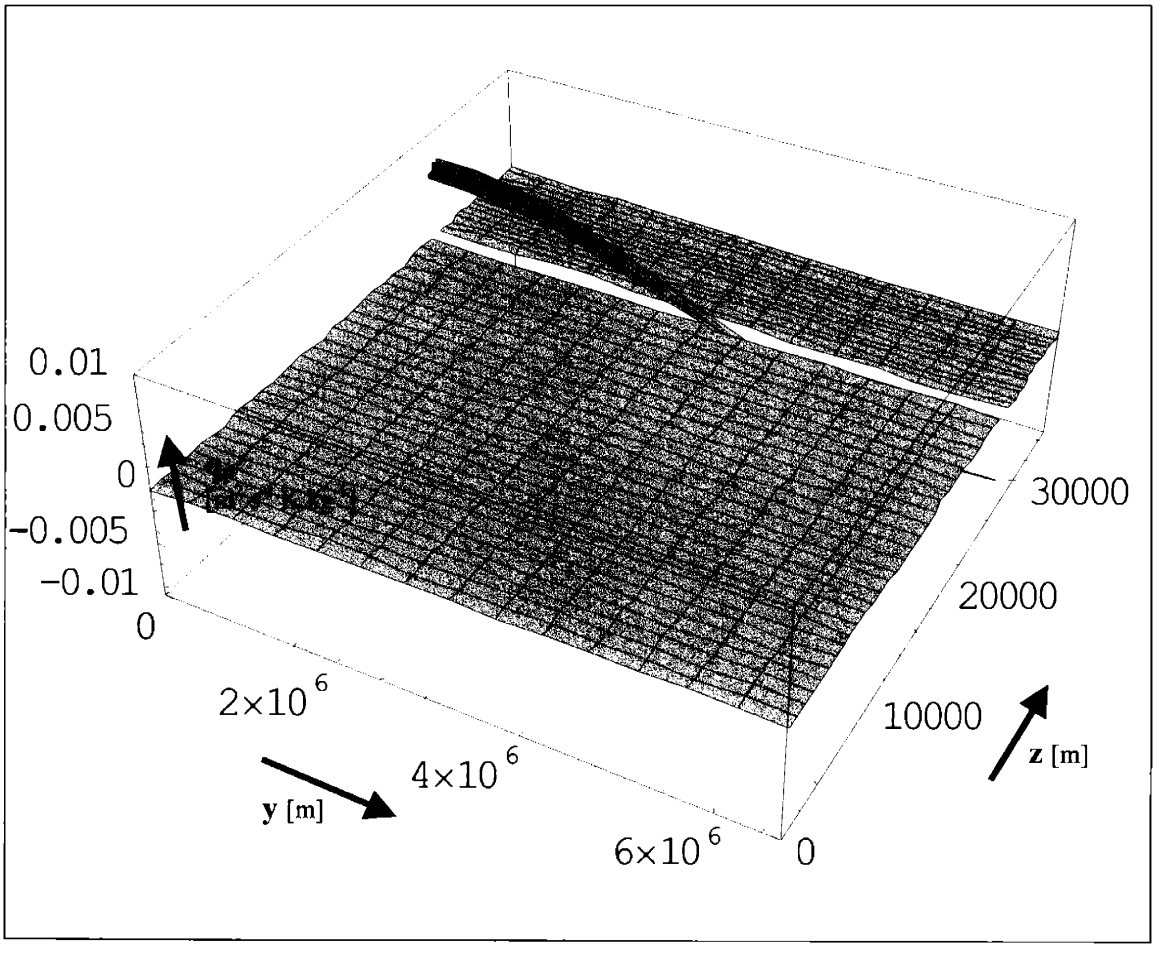

Figure 20. PV anomaly field (q_p') for 26-27 km layer

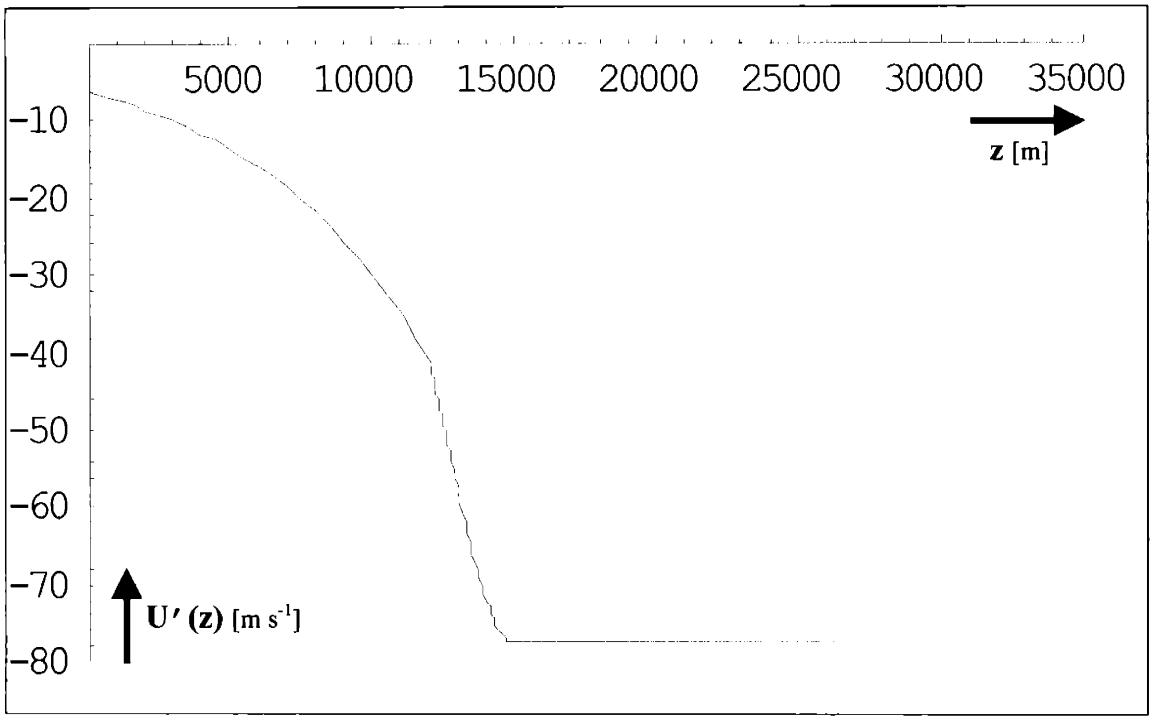

Figure 21. Zonal wind anomaly height profile ($U'(z)$) for 13-15 km layer

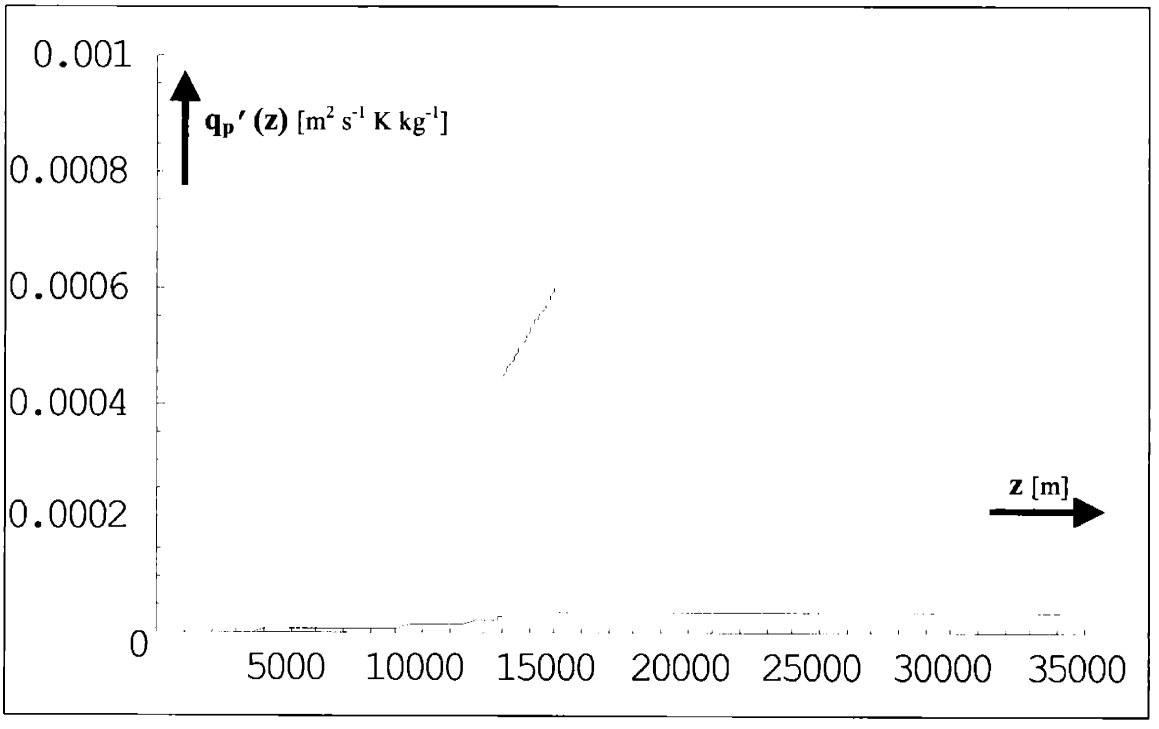

Figure 22. PV anomaly height profile ($q_p'(z)$) for 13-15 km layer

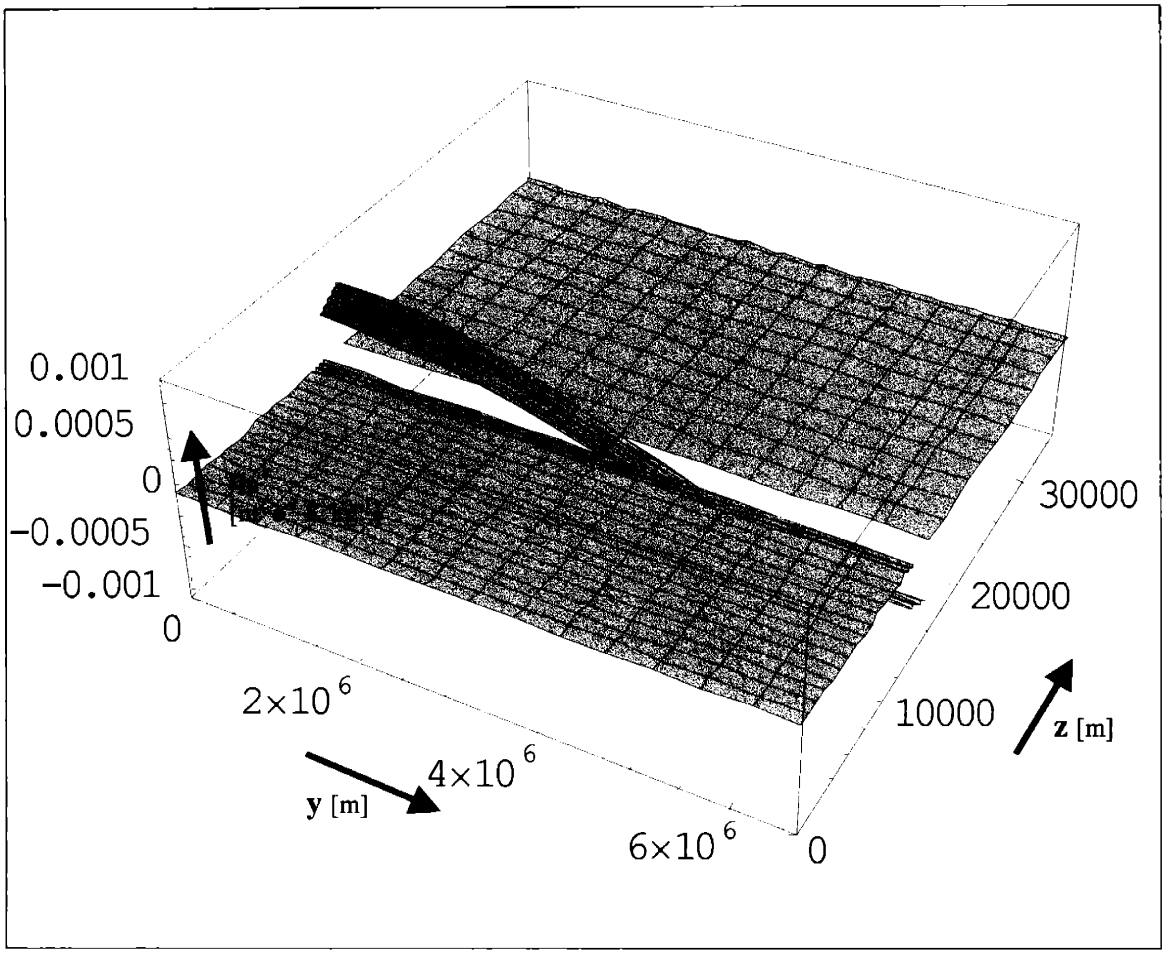

Figure 23. PV anomaly field (q_p') for 13-15 km layer

The basic shape of the perturbation zonal wind height profile remains the same throughout for all three selected layers. Above the selected layer of dissipation, the zonal wind is constant with height, which is a result of the fact that the wind shear is zero here (Equation 39). The sharpest increase in the magnitude of the perturbation zonal wind with height occurs within the layer of wave dissipation. This may be understood through piecewise PV inversion. Since it is in the layer of dissipation that the upward propagating surface waves deposit all of their momentum, this is where the anomalous PV is greatest,

and this can easily be seen to be true in the above plots of q_p'. By the electrostatics analogy, the closer an area is to the region of PV being inverted, the greater the associated non-local effect will be. Therefore, the layer where the perturbation PV magnitude is the greatest is also where the associated anomalous zonal wind is largest, and this is why the magnitude of the perturbation zonal wind increases the most rapidly in the layer of wave dissipation. Below the layer of dissipation, the magnitude of the anomalous zonal wind decreases exponentially downward from the value it possessed at the lower boundary of the layer until it reaches the fixed value given in Equation 44 at the surface.

While the perturbation zonal wind height profile is a continuous function, a result of the fact that the geopotential height is continuous (Equation 2), the PV perturbation height profile is not continuous, and is not required to be so by definition (Equation 3). It is evident from the perturbation PV height profiles and PV anomaly fields that the magnitude of the anomalous PV is small everywhere except for in the layer of wave dissipation. This is the case for all three selected layers. As explained in the preceding paragraph, this result is not unexpected due to the fact that the largest anomalous PV is expected to be in the region of maximum momentum deposition. Since in this case the region with the greatest momentum deposition has been constructed to be the layer where the upward propagating surface waves are specified to completely dissipate, this is where the PV is expected to be greatest and this is confirmed in the preceding Figures 16, 19, and 22.

To some extent, the shape of the calculated PV profile here in the stationary solution resembles the specified height profile of the anomalous PV in the transient case, in

that the PV has a large discontinuous maximum in the layer of dissipation. However, unlike the transient solution, the stationary perturbation PV is not zero outside the layer of dissipation, even though it is significantly small relative to the magnitude it possesses in the layer. Also, the PV magnitude within the layer of dissipation is not constant with height in the stationary case, while it was specified to be so in the transient case. One reason behind the differences in the two cases has to do with the fact that, while the atmosphere was assumed to be adiabatic in the transient solution, in the stationary case Newtonian cooling was assumed. The differences also stem from the somewhat reversed construction of the stationary solution model as compared to the transient model. In the stationary case, it was the product of the poleward PV flux and reference density that was specified to be zero everywhere except for in the layer of dissipation, while in the transient case it was the value of the perturbation PV itself that was specified as such. However, it is still of interest to note that in both the transient and stationary models, the perturbation PV possesses a discontinuous maximum throughout the height of the wave dissipation layer and is zero or nearly zero everywhere else above and below this layer. This leads to the determination that the height in the stratosphere at which the induced surface waves dissipate is of great importance in determining the magnitude of the associated effect the stratosphere has at the surface as a result of the PV redistribution caused by the breaking waves. Therefore, the results here indicate that in using piecewise PV inversion to deduce the magnitude of the effect of the stratosphere on the surface, it is only the layers in which significant wave dissipation is occurring that need be inverted in order to obtain a reasonably complete picture of the surface signal.

In assessing the effect that the height of wave dissipation has at the surface, the results of the 13-14 km layer (Figures 15-17) compared to the 26-27 km layer (Figures 18-20) reveal that the magnitude of the perturbation PV is much larger in the higher layer than in the lower layer. As constructed, both layers are required to yield the same fixed value of perturbation zonal wind at the surface. Therefore, it may be concluded that the higher the perturbation PV layer is in the stratosphere, the larger the magnitude of the PV must be in order for the associated surface signal to have the same strength. This may be understood through the electrostatics analogy, that the anomalous PV must possess an increasingly larger magnitude the higher it is in the stratosphere in order for its associated non-local effect to still have the same magnitude at the surface. Alternatively, the greater PV magnitude in the higher layer can be seen as a result of the fact that as the surface waves propagate upwards, their amplitude increases exponentially as the density of the atmosphere decreases. Or equivalently, because the two layers are of equal thickness but significantly different heights, the higher layer possesses a much smaller mass by volume than the lower layer. Since the surface wave flux remains fixed in both cases, the momentum deposited in each layer is the same. Consequently, the wave momentum deposition into the smaller mass of the upper layer yields a larger magnitude PV anomaly than for the lower layer.

Note also that in the case of the higher layer, the perturbation zonal wind is much larger than it is for the lower layer, and in fact becomes unrealistically large higher up in the atmosphere. This is due to the fact that here in the model, it has been assumed that the surface waves entirely dissipate in a finite stratospheric layer regardless of the height of

that layer. However, in the real atmosphere the upward propagating waves would not be able to completely dissipate in a finite atmospheric layer if the height of that layer was sufficiently high in the atmosphere to then have a mass that was too small to accommodate the dissipation of all the upward propagating waves. Then in the real atmosphere, these excess waves would be reflected back down toward the surface again. Therefore, it is the lack of realistic wave dynamics in the model that is primary responsible for the presence of the unrealistic values of anomalous zonal wind.

Now the effect of the thickness of the dissipation layer will be examined for the stationary case through a comparison of the 13-14 km layer (Figures 15-17) and the 13-15 km layer (Figures 19-21). Below the layer of dissipation, the PV anomaly height profiles for both layer thicknesses are identical, and only marginally different above the layer of dissipation. However, within the one kilometer dissipation layer, the magnitude of the perturbation PV is approximately double what it is in the two kilometer layer. The reason the PV anomaly height profiles primarily only differ within the layer of dissipation stems from the construction of the model, that the surface waves are required to dissipate solely within the dissipation layer. The approximate doubling of PV magnitude within the thinner layer of dissipation versus the thicker layer has to do with the fact that the quantity of momentum deposited by the fixed constant surface wave flux is the same for both the one and two kilometer thick layers. This means that the fixed constant momentum deposited in the 13-14 km layer is compressed into half the volume it was in the 13-15 km layer, and thus the approximately twice as large associated PV anomaly magnitude. The reason the PV magnitude of the one kilometer layer is not exactly double that of the two

kilometer layer, approximately 9 x 10^{-4} m^2 s^{-1} K kg^{-1} in the 13-14 km layer versus 5 x 10^{-4} m^2 s^{-1} K kg^{-1} in the 13-15 km layer, is because the average height of the 13-15 km layer is slightly higher in the stratosphere than the 13-14 km layer. By the electrostatics analogy, the magnitude of the perturbation PV in the 13-15 km layer must therefore be slightly larger here than if it was at the same average height as the 13-14 km layer in order to have the same magnitude associated surface signal.

The zonal wind height profiles of both layers are identical from the surface upward to 14 km at the top of the one kilometer thick layer. Above this height, the perturbation zonal wind is constant for the 13-14 km layer, but continues to grow between 14-15 km for the 13-15 km layer. This results in a constant value of zonal wind anomaly of −67.25 m s^{-1} for the 13-14 km layer versus −77.60 m s^{-1} for the 13-15 km layer for the infinite regions above the layers of dissipation. It is the discrepancy in average height between the two layers that is responsible for the slightly higher constant value of perturbation zonal wind above the upper boundary for both layers. The relative magnitude of the perturbation PV in the 13-15 km layer is larger for its overall volume than that of the 13-14 km layer. Therefore, the inversion of the PV in the 13-15 km layer will result in a slightly larger magnitude perturbation zonal wind value by the top of the dissipation layer and thus in the infinite region above the layer as well. It may therefore be presumed that as long as the dissipation layer maintains a constant average height in the stratosphere, then an increase in the thickness of the layer will result in an inversely proportionate decrease in the PV anomaly magnitude of that layer, but no change to the height profile of the perturbation zonal wind.

Note that due to the construction of the stationary model, the overall results here may only offer insight into the dynamics of the stratosphere-surface link, and no actual quantification may be made of how wave dissipation height and layer thickness impact the surface, as could be done in the transient case. Therefore, from the results shown by the method of piecewise PV inversion here in the stationary solution model, the following conclusions may be made. For a fixed constant surface eddy flux of solely vertically propagating topographically forced waves, the level in the stratosphere at which these waves dissipate is where there will be a significant discontinuous maximum in anomalous PV. Except for within the layer of wave dissipation, the perturbation PV is near to zero elsewhere in the atmosphere. Therefore, if using the method of piecewise PV inversion to diagnose the stratospheric PV signal in surface climate, inversion of the PV within the dissipation layer alone should be sufficient to give a solution at the surface that is very nearly complete. This knowledge may allow surface climate models to include simulation of the stratospheric effect on surface climate with minimal computational costs while still maintaining accuracy. Also, as long as the steady-state surface wave flux remains fixed and constant, then the value of the perturbation zonal wind at the surface will also remain fixed and constant. While this is known to be the case, then the height in the stratosphere at which these waves dissipate will cause the resulting anomalous PV to be larger the higher the dissipation level is. The thickness of the layer of dissipation has no effect on the corresponding height profile of perturbation zonal wind as long as the average height of the layer remains the same. However, the thicker the dissipation layer becomes, the proportionately inversely smaller the average magnitude of the anomalous PV will become

in the layer. The value of the fixed constant surface wave flux as given through the vertical component of the Eliassen-Palm flux at the surface was calculated for typical steady-state atmospheric values. The associated magnitude of surface zonal wind for this realistic wave flux is significant, of the order of several meters per second. Therefore, in the case where the magnitude of the surface wave flux is not predetermined, if it is known where these waves ultimately dissipate, if in some layer in the stratosphere, then the resulting perturbation in PV may be piecewise inverted to give the associated, and presumably significant, surface climate signal. Thus, as in the transient case, the results of the stationary solution also indicate that there is a significant link between the stratosphere and the surface.

VII. SUMMARY AND CONCLUSIONS

The associated effect of the stratosphere on the surface has been examined in both the transient and stationary cases using the method of piecewise PV inversion. One motivation behind these studies was to be able to make a determination of whether the stratosphere had a significant signal at the surface in either, or both, the instantaneous or time-averaged cases. Such a determination allows an assessment to be made as to whether the inclusion of stratospheric dynamics in models attempting to forecast surface weather or simulate surface climate would significantly improve their accuracy, or if instead the inclusion of a modeled stratosphere would simply be computationally costly without resulting in a significant improvement in accuracy. Another motivation behind performing these studies was to examine the dynamical interaction between the stratosphere and the

surface in the hopes of being able to shed additional light on the subject of downward communication in the atmosphere, since it is a subject that is still not well understood. In addition, examination of the dynamics of the stratosphere-surface link also has the potential to reveal whether certain aspects of the dynamical interaction have greater importance than others. Consequently, if the link between the stratosphere and surface is deemed to be significant, such knowledge would allow surface models to simulate only the most relevant stratosphere-surface dynamics in order to minimize computational costs.

In the transient solution model, the associated effect of the stratosphere on the surface was examined for short time-scales during a simulated major stratospheric warming event. This allowed an assessment to be made of how and to what extent the stratosphere factors in determining the weather at the surface of the earth. The model was constructed such that the anomalous PV was zero everywhere in the atmosphere and at the surface except for in an infinite layer above an arbitrary level in the stratosphere. Piecewise PV inversion was then performed on this arbitrary infinite layer of anomalous PV in order to obtain the general solutions for the associated perturbation zonal wind and temperature fields throughout the atmosphere and at the surface. Because the model was solved under the assumption of QG, any linear combination of the infinite layers of anomalous PV could then be constructed in order to give the inverted solutions at the surface and through the atmosphere for any finite layer of anomalous PV in the stratosphere.

In the first case studied in the transient solution, a constant fixed value of anomalous PV was moved to different levels in the stratosphere in order to diagnose the

effect that PV anomaly height has on the strength of the inverted associated signal at the surface. It was determined that as the height of the fixed constant PV anomaly is raised, its associated signal at the surface in terms of perturbation zonal wind decreases exponentially in response. This exponential decrease in the surface signal may be understood through the electrostatics analogy, that the non-local effect at the surface of the stratospheric PV anomaly decreases in strength as the PV anomaly is increasingly further removed from the surface. It was concluded that, for a reasonable value of perturbation PV, the stratosphere does have a significant associated signal at the surface in terms of anomalous zonal wind, and that it is primarily the lower stratosphere that has the largest significant associated effect at the surface.

In the second case studied in the transient solution, a fixed constant surface flux of vertically propagating waves was induced in the model. These waves were assumed to have been topographically forced for example, so that there was no anomalous PV associated with the formation of these waves at the surface in order to comply with the construction of the model and also to keep the stratospheric PV inversions straightforward. The surface waves were then specified to propagate up into the stratosphere to a certain level, above which they were presumed to completely dissipate. Changing the level above which these waves dissipated resulted in different values for the perturbation PV. The anomalous PV was then inverted for each of the infinite layers and the associated surface anomaly fields solved for. Subtraction of these results gave the surface solutions for wave dissipation occurring in stratospheric layers of finite thickness. From this study, it was shown that as the height at which the surface waves are specified to dissipate is raised, the

resulting anomalies in PV increase exponentially while the associated inverted solution for surface perturbation zonal wind field decrease exponentially. The reason behind this has to do with the fact that while the magnitude of the PV anomaly increases exponentially as the height of dissipation is raised, attributed to the decrease in atmospheric density with height, it is not enough to offset the concurrent decrease in the non-local effect of the PV anomaly at the surface as its distance from the surface increases, by the electrostatics analogy. Nonetheless, the associated signal at the surface of the anomalous stratospheric PV induced by the dissipation of the surface waves is significant. Again, the lower the height is in the stratosphere at which the surface waves dissipate, the larger the associated surface signal is.

It may be concluded in the transient case that the stratosphere does have a significant associated effect at the surface during a major stratospheric warming. To avoid significant error, surface weather forecasting models should therefore include adequate simulation of this stratosphere-surface link. The results of the transient case study also indicate that simulation of the lower stratosphere alone may be sufficient in representing the stratosphere as a whole in order to minimize computational costs while still maximizing the accuracy of the model. Although, it must be noted that, in turn, the dynamics of the lower stratosphere may well depend significantly upon the dynamics of the atmosphere above.

The stationary solution model allowed the stratosphere-surface link to be examined in the time-averaged steady-state atmosphere, so that the effect of the stratosphere on surface climate could be assessed. The model was constructed with a fixed constant

surface wave flux, also assumed to be forced by topography for example, which was assumed to dissipate in an arbitrary finite layer in the stratosphere. The time-averaged state of the stationary solution model atmosphere means that frictional wave drag at the surface is significant. Therefore, the value of the surface perturbation zonal wind is solely determined by the magnitude of the surface wave flux. Consequently, in this case inversion of the PV for different stratospheric layers always returns the same fixed constant value for the perturbation zonal wind at the surface. Therefore, the stratosphere-surface link was instead assessed through an examination of how the height profiles of perturbation PV and zonal wind changed with the choice of dissipation layer.

In the stationary case, it was first examined how dissipation layer height impacts the dynamics of the stratosphere-surface link. Comparison of two layers of equal thickness but significantly different stratospheric heights revealed that the equal momentum deposition in both layers resulted in a significantly larger PV anomaly in the higher layer than in the lower layer. This is due to the decreasing density with height in the atmosphere, and agrees with the transient case that a PV anomaly must increase in magnitude as it is further removed from the surface if it is to still possess the same constant value non-local effect there.

Next in the stationary case, it was examined how dissipation layer thickness impacted the dynamical interaction between the stratosphere and the surface. A comparison of two layers of different thickness and approximately equal height yielded the following results. For the complete dissipation of a fixed constant surface wave flux in a layer that maintained the same average height but changed in thickness, the resulting

magnitude of perturbation PV decreased inversely proportionately as the layer thickness increased. On the other hand, the perturbation zonal wind height profile essentially remained unchanged. Only the shape of the profile changed slightly as the layer thickness was changed, the constant value of perturbation zonal wind above the layer remained the same.

Therefore, in the stationary solution it may also be concluded that the link between the stratosphere and the surface is significant, due to the fact that the results were determined using a realistic value for the steady-state surface wave flux. Consequently, models attempting to accurately simulate surface climate must include the stratospheric dynamics discussed here. In all of the studies performed here in the stationary case, the PV always possessed a significant discontinuous maximum within the layer of dissipation, and was near zero everywhere else. Therefore, if simulating the stratosphere-surface dynamics through piecewise PV inversion, then only the stratospheric layer of dissipation need be inverted in order to obtain a reasonably accurate picture of the associated effect of the stratosphere on surface climate.

Thus, while PV inversion does not allow for a direct determination of cause and effect, it may nonetheless be concluded from the results shown here that the stratosphere does possess a significant associated effect at the surface, both in terms of surface weather and climate. This link between the stratosphere and the surface may also be considered to be relatively robust, as it has been shown here to be evident and significant in both the instantaneous time-scales of the transient case and the time-averaged state of the stationary solution. In conclusion, any models which are attempting to accurately forecast surface

weather or simulate surface climate must include an adequate representation of the dynamics presented here between the stratosphere and the surface.

BIBLIOGRAPHY

Baldwin, M. P.: The Arctic Oscillation and its role in stratosphere-troposphere coupling, *SPARC Newsletter*, **14**, 10-14, 2000.

Baldwin, M. P., X. Cheng and T. J. Dunkerton: Observed correlations between winter-mean tropospheric and stratospheric circulation anomalies, *Geophysical Research Letters*, **21**, 1141-1144, 1994.

Baldwin, M. P. and T. J. Dunkerton: Propagation of the Arctic Oscillation from the stratosphere to the troposphere, *Journal of Geophysical Research*, **104**, 30,937-30,946, 1999.

Baldwin, M. P. and T. J. Dunkerton: Stratospheric Harbingers of Anomalous Weather Regimes, *Science*, **294**, 581-584, 2001.

Bishop, C. and A. Thorpe: Potential vorticity and the electrostatics analogy: Quasi-geostrophic theory, *Quarterly Journal of the Royal Meteorological Society*, **120**, 713-731, 1994.

Black, R. X.: Stratospheric Forcing of Surface Climate in the Arctic Oscillation, *Journal of Climate*, **15**, 268-277, 2002.

Charney, J. G. and P. G. Drazin: Propagation of Planetary-Scale Disturbances from the Lower into the Upper Atmosphere, *Journal of Geophysical Research*, **66**, 83-109, 1961.

Davis, C. A. and K. A. Emanuel: Potential Vorticity Diagnostics of Cyclogenesis, *Monthly Weather Review*, **119**, 1929-1953, 1991.

Davis, C. A.: Piecewise Potential Vorticity Inversion, *Journal of the Atmospheric Sciences*, **49**, 1397-1411, 1992.

Hartley, D. E., J. T. Villarin, R. X. Black, and C. A. Davis: A new perspective on the dynamical link between the stratosphere and troposphere, *Nature*, **39**, 471-474, 1998.

Hurrell, J. W.: Decadal Trends in the North Atlantic Oscillation: Regional Temperatures and Precipitation, *Science*, **269**, 676-679, 1995.

James, I. N.: *Introduction to Circulating Atmospheres*. Cambridge University Press, New York, 422 pp., 1994.

Kerr, R. A.: Getting a Handle on The North's 'El Niño', *Science*, **294**, 494-495, 2001.

Kodera, K., K. Yamazaki, M. Chiba and K. Shibata: Downward propagation of upper stratospheric mean zonal wind perturbation to the troposphere, *Geophysical Research Letters*, **17**, 1263-1266, 1990.

Kuroda, Y. and K. Kodera: Role of planetary waves in the stratosphere-troposphere coupled variability in the Northern Hemisphere winter, *Geophysical Research Letters*, **26**, 2375-2378, 1999.

Peixoto, J. P. and A. H. Oort: *Physics of Climate*. Springer-Verlag, New York, 520 pp., 1992.

Perlwitz, J. and H.-F. Graf: The Statistical Connection between Tropospheric and Stratospheric Circulation of the Northern Hemisphere in Winter, *Journal of Climate*, **8**, 2281-2295, 1995.

Plumb, R. A. and K. Semeniuk: Downward migration of extratropical zonal wind anomalies, *Journal of Geophysical Research*, **108**, art. no. 4223, 2003.

Thompson, D. W. J. and J. M. Wallace: The Arctic Oscillation signature in the wintertime geopotential height and temperature fields, *Geophysical Research Letters*, **25**, 1297-1300, 1998.

Thompson, D. W. J. and J. M. Wallace: Annular Modes in the Extratropical Circulation. Part I: Month-to-Month Variability, *Journal of Climate*, **13**, 1000-1016, 2000.

Thompson, D. W. J. and J. M. Wallace: Annular Modes in the Extratropical Circulation. Part II: Trends, *Journal of Climate*, **13**, 1018-1036, 2000.

Wallace, J. M.: North Atlantic Oscillation/Annular Mode: Two Paradigms - One Phenomenon, *Quarterly Journal of the Royal Meteorological Society*, **126**, 791-805, 2000.

Wallace, J. M. and D. W. J. Thompson: Annular Modes and Climate Prediction, Physics Today, 55, 28-33, 2002.